

Impact of leakage to the dynamic of a ST_0 qubit implemented on a Double Quantum Dot device

Javier Oliva del Moral,^{1,2,*} Olatz Sanz Larrarte,¹ Reza Dastbasteh,¹ Josu Etxezarreta Martinez,^{1,3} and Rubén M. Otxoa^{4,†}

¹*Department of Basic Sciences, Tecnum - University of Navarra, 20018 San Sebastián, Spain.*

²*Donostia International Physics Center, 20018 San Sebastián, Spain.*

³*Visiting Researcher at the Cavendish Laboratory, Department of Physics, University of Cambridge, Cambridge CB3 0HE, UK.*

⁴*Hitachi Cambridge Laboratory, J. J. Thomson Avenue, Cambridge CB3 0HE, United Kingdom.*

Spin qubits in quantum dots are a promising technology for quantum computing due to their fast response time and long coherence times. An electromagnetic pulse is applied to the system for a specific duration to perform a desired rotation. To avoid decoherence, the amplitude and gate time must be highly accurate. In this work, we aim to study the impact of leakage during the gate time evolution of a spin qubit encoded in a double quantum dot device. We prove that, in the weak interaction regime, leakage introduces a shift in the phase of the time evolution operator, causing over- or under-rotations. Indeed, controlling the leakage terms is useful for adjusting the time needed to perform a quantum computation. This is crucial for running fault-tolerant algorithms and is beneficial for Quantum Error Mitigation techniques.

I. INTRODUCTION

Quantum Dots (QD) hosting spin qubits are an innovative technology for building quantum computers leveraging the spin state of electrons confined in semiconductor nano-structures. These QDs are created by gate electrodes patterned on top of a semiconductor which induce a confining potential for electrons[1]. The number of electrons can be controlled by manipulating the applied potential[2]. The spin of the electron serves as quantum bit unit and can be manipulated by applying external electric and magnetic fields. When an external magnetic field is applied perpendicular to the plane of the QD, the energy of the degenerate $|\uparrow\rangle$ and $|\downarrow\rangle$ states is split due to the Zeeman interaction so that they can be used as the computational basis where the qubit is encoded. Other alternatives exist for encoding a qubit using more than a single QD, including singlet-triplet spin qubits and flip-flop qubits, among others[1]. Key features of spin qubits in QDs are their rapid response time to external electric and magnetic fields resulting in fast quantum gates and long coherence times[3]. As a result, they stand as a promising technology for developing quantum computers. However, several technological challenges related to control, scalability, and connectivity must be overcome to make such proposal a reality. The control needed to perform qubit rotations depends on various factors such as: the encoding protocol, the interaction strength, the inherent properties of the used semiconductor and the dimensionality of the QD[1]. Consequently, a crucial aspect of spin qubit manipulation is the fidelity achieved when performing qubit rotations by means of external electric and/or magnetic fields. This

issue is of paramount importance as running quantum algorithms typically requires a large number of rotations or quantum gates, each of which must be highly precise to prevent coherent errors arising from under- or over-rotations[4]. Incoherent errors arising from the decoherence of the quantum information as result of its interaction with the environment is also an important issue and unavoidably leads to imprecise results[5–7]. To circumvent this problem, Quantum Error Mitigation (QEM) techniques[6], such as zero-noise extrapolation (ZNE), aim to enhance the accuracy of quantum algorithms by post-processing several noisy measurements of expectation values of interest[7, 8]. These methods provide a promising strategy for harnessing useful outcomes from quantum computers in the noisy intermediate-scale quantum (NISQ) era until the development of fault-tolerant quantum processors. Fault-tolerant quantum computing refers to the paradigm of being able to reliably perform quantum computations even if its constituent elements are imperfect. The building block of such machines is the so-called quantum error correction (QEC). Despite recent breakthrough advances in this field, such as the experimental demonstration on a superconducting qubit chip that surface codes can suppress the error rate when operating at sub-threshold error rates[9], it has not yet been proven that a universal fault-tolerant quantum computers can be constructed with current technology. The main challenges are related to qubit connectivity as well as the challenge of achieving a universal set of quantum gates for the logical qubits encoded on stabilizer codes[10], reaching physical error rates below the threshold for certain technologies [11] and real-time decoders[5], among others.

Therefore, it is essential to fabricate qubits with long coherence times and to implement high-fidelity gates, measurements and state preparations. In this paradigm, a key challenge related to gate implementation is design-

* jolivam@unav.es

† ro274@cam.ac.uk

ing accurate pulses to prevent over- or under-rotations (coherent errors) and optimize timing, since faster gates may result in lower incoherent errors[12]. Furthermore, the systems in which qubits are encoded may not be strictly two-level systems, i.e. more energy levels than the computational subspace (where the qubit is encoded) may exist and be accessible. The presence of those other levels introduces extra transitions or pathways between qubit states, potentially altering their dynamics[13]. In this study, we investigate how these additional states affect the quantum time evolution operators when a constant pulse is applied over time. Interestingly, this corresponds to a scenario that can be tested experimentally with certain ease. We focus on singlet-triplet (ST₀) qubits encoded in a double quantum dot (DQD) device, as they offer more than two accessible levels, and transitions between these levels can be manipulated at will by means of external fields. However, the theoretical approach we present is generalizable to any qubit technology with more than two accessible energy levels.

The article is organized as follows: Section II provides an introduction to the quantum time evolution operator and the physics of QD and DQD systems, including an overview of how rotations are implemented in these platforms. Next, Section III focuses on ST₀ qubits, where the logical states are encoded in the singlet and neutral states of the DQD. The study concludes with Section IV, which offers a discussion, and Section V, which presents the conclusions along with a brief discussion of quantum system time evolution in the presence of leakage.

II. THEORETICAL BACKGROUND

The dynamics of a quantum system is described by its Hamiltonian, which defines the energies of the different possible states and the transitions among them. The time-evolution operator is obtained from the time-dependent Schrödinger equation:

$$\frac{d|\psi(t)\rangle}{dt} = -\frac{i}{\hbar}H|\psi(t)\rangle, \quad (1)$$

where \hbar is the Planck constant and $\psi(t)$ is the wavefunction. The Hamiltonian can be diagonalized, i.e. $H = \sum_j \lambda_j |\varphi_j\rangle\langle\varphi_j|$, where $\{\lambda_j\}$ are the eigenvalues or energies associated to the eigenstates $\{|\varphi_j\rangle\}$. Any state $|\psi(t)\rangle$ over such system can be represented as a superposition of the eigenstates of the Hamiltonian, $\{\varphi_j\}$, with associated amplitudes, $\{\alpha_j\}$. Then, the solution of the Eq. 1 has the following form:

$$|\psi(t)\rangle = \hat{U}(t, 0)|\psi(0)\rangle = \sum_j \alpha_j \exp(-i\lambda_j t/\hbar) |\varphi_j\rangle, \quad (2)$$

where the unitary evolution operator $\hat{U}(t, t_0)$ is defined as

$$\hat{U}(t, t_0) = \sum_j \exp(-i\lambda_j(t - t_0)/\hbar) |\varphi_j\rangle\langle\varphi_j|. \quad (3)$$

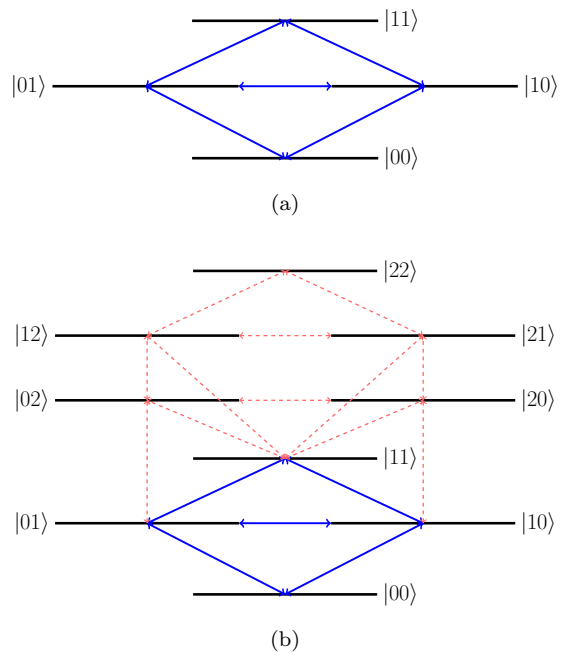


FIG. 1. Graphical representation of the possible states of (a) an ensemble of two TLSs (or qubits) and (b) an ensemble of two three level systems (or qutrits) with the transitions between the states (blue and red lines). The energy of each state is given by the respective diagonal term of the Hamiltonian, H_0 , and the transitions are related to the off-diagonal terms of the Hamiltonian, H_I . Blue (solid) lines represent rotations of the qubit, i.e. in the SU(2) subspace, and red (dashed) lines represent leakage transitions to higher energy levels and between them.

Note from the previous expression that, the higher the energy of an eigenstate, the faster its time evolution will be. In the interaction picture, the Hamiltonian is split in the non-interaction or diagonal terms H_0 and the interaction or off-diagonal terms H_I . In this picture, the evolution from an initial state to a final state is given by the unitary time evolution operator $\hat{U}_I(t, t_0)$:

$$\hat{U}_I(t, t_0) = \exp(\Gamma(t - t_0)), \quad (4)$$

where Γ is related to the possible interactions (or paths) from an initial state $|\psi_{\text{In}}\rangle$ to a final state $|\psi_{\text{Out}}\rangle$ and it is proportional to the probability of the transition:

$$\Gamma \propto |\langle\psi_{\text{Out}}|H_I|\psi_{\text{In}}\rangle|^2. \quad (5)$$

The terms that conform H_I determine how a state at time t_0 will evolve to other state at time t . For example, in a two-level system (TLS), the transition from an initial state to a final state is uniquely defined by the direct transition, meaning there is only one possible path from $|0\rangle$ to $|1\rangle$. For an ensemble of two TLSs, when we apply a rotation the possible transitions are represented by blue lines in Fig. 1a. However, whenever more accessible levels with allowed transitions among them exist, the evolution

between the states becomes more complex. A graphical representation of an ensemble of two quantum systems with three accessible levels, i.e. qutrits, and transitions among these levels is shown in Fig. 1b. Blue (solid) lines represents rotations of the qubit and red (dashed) lines represents leakage transitions to higher energy levels. Note that we consider that qubits are encoded in those three level systems (depicted in blue in Fig. 1b), but the other levels out of the computational subspace are still accessible (depicted in red in Fig. 1b). The difference in how these two scenarios evolve over time is the main question we analyze in this paper, i.e. a strictly two-level system qubit versus a qubit encoded in a higher dimensional quantum state.

Generally, a qubit encoded on a two-level system is defined by a 2×2 Hamiltonian:

$$H_0 = \begin{pmatrix} \lambda_0 & 0 \\ 0 & \lambda_1 \end{pmatrix}, \quad (6)$$

hence, the free evolution of the qubit is determined by λ_0 and λ_1 . To perform a rotation, defined as, $R_i(\theta)$, of θ radians around $i \in \{\hat{x}, \hat{y}, \hat{z}\}$, we have to add an interaction term H_I to Eq. 6, which belongs to the same Hilbert space, defined by the Pauli matrices σ_x , σ_y or σ_z , respectively:

$$R_i(\theta) = \exp\left(-i\sigma_i \frac{\theta}{2}\right), \quad (7)$$

where $\sigma_i \in \{\sigma_x, \sigma_y, \sigma_z\}$. Generally, this interaction term is enforced to the system by means of an external pulse applied to it. Importantly, since the applied pulses cannot have arbitrary shapes, we will assume that rectangular shapes are used for enforcing these rotations, which are more feasible to be implemented experimentally.

While considering a qubit as a strict TLS is a useful abstraction, real quantum systems often include more possible energy levels that can be accessed. A qubit is encoded using two of those levels, defining a computational subspace. Ideally, transitions from the computational basis, defined by a 2×2 Hamiltonian (Eq. 6), to higher energy states are considered to be prohibited. However, a direct consequence of the existence of those extra accessible levels is that the qubit leaves the computational basis $|0\rangle$ and $|1\rangle$. This effect is known as *leakage* [13–16]. The existence of leakage makes the number of possible paths from an initial state to a final state to increase (as it is illustrated in Fig. 1b), thus, changing the time evolution operator. The Hamiltonian of a quantum system with more than two levels is given by matrix formed by the computational basis H_0 (Eq. 6); the Hamiltonian of higher energy states outside the computational space H_{out} ; and Hamiltonian which defines the probabilities of transitions between both spaces H_{leak} :

$$H = \begin{pmatrix} H_0 & H_{\text{leak}} \\ H_{\text{leak}}^\dagger & H_{\text{out}} \end{pmatrix}, \quad (8)$$

If we consider n as the number of energy levels, then H is a $n \times n$ matrix, H_0 is a 2×2 matrix, H_{leak} is a $2 \times (n-2)$ matrix and H_{out} is a $(n-2) \times (n-2)$ matrix. In the case of $n = 3$ (three level system) the Hamiltonian would be given by:

$$H = \hbar \begin{pmatrix} \lambda_0 & 0 & \mu_1 \\ 0 & \lambda_1 & \mu_2 \\ \mu_1^* & \mu_2^* & \lambda_2 \end{pmatrix}, \quad (9)$$

where $H_{\text{leak}} = \begin{pmatrix} \mu_1 \\ \mu_2 \end{pmatrix}$ and $H_{\text{out}} = (\lambda_2)$, being λ_2 the energy of the state outside the computational space, referred to as $|2\rangle$. Fig. 1b represents the possible transitions of an ensemble of two of them. In the following section, we present how qubits are encoded in a QD or in a DQD device, which has more than two accessible levels, implying that leakage affects the dynamics.

A. Spin Qubits in Quantum Dots

QDs are created on semiconductors interfaces, where a small empty region is created in the 2 dimensional electron gas (2DEG) by applying an external potential V_{ext} . There are many heterostructures used to generate a 2DEG, where QDs can be created, such as Gallium arsenide (GaAs) and aluminum gallium arsenide (AlGaAs)[17–19]; Silicon-Silicon Dioxide (Si/SiO₂) or silicon Germanium (SiGe)[20, 21]. Nowadays, heterostructures based on purified silicon (²⁸Si) are taking a lot of attention because its spinless nucleus, i.e. there is not hyperfine interaction between them and an electron inside a QD[3, 22].

By controlling the external potential V_{ext} , the drain potential V_d and the source potential V_s , which are the potentials which control the barrier between the QD and the 2DEG; we can change the charge energy to load electrons inside the QD [23]. A qubit is usually encoded on a QD charged with a single electron, while an external magnetic field is applied to split the degenerate energies of the spin states $|\uparrow\rangle \equiv |1\rangle$ and $|\downarrow\rangle \equiv |0\rangle$ due to the Zeeman interaction, forming the computational basis. The Zeeman interaction Hamiltonian $H_Z(t)$ is given by:

$$H_Z(t) = g\mu_B \mathbf{B}(t) \cdot \mathbf{s}, \quad (10)$$

where g is the gyromagnetic ratio of the electron, μ_B is the Bohr magneton, \mathbf{B} is the external magnetic field and \cdot refers to the dot product. $\mathbf{s} = \frac{1}{2}\boldsymbol{\sigma}$ is the spin operator vector, with $\boldsymbol{\sigma} = \{\sigma_x, \sigma_y, \sigma_z\}$ the vector of Pauli matrices. Those matrices correspond to the generators of the SU(2) Lie algebra. To generate the qubit, we apply a constant external magnetic field in the \hat{z} direction, i.e. $\mathbf{B} = (0, 0, B_z)$. Then, the qubit Hamiltonian is given by:

$$H_{QD} = g\mu_B \begin{pmatrix} B_z/2 & 0 \\ 0 & -B_z/2 \end{pmatrix}. \quad (11)$$

To control the state of the system, i.e. to apply quantum gates to a single qubit, external time-varying magnetic fields are applied in the direction we want to rotate the qubit, $\mathbf{H}_C(\mathbf{B}(t))$. The total Hamiltonian of the system, accounting for both the qubit dynamics and the external controls, is given by:

$$\mathbf{H}_{QD} + \mathbf{H}_C(t) = \frac{1}{2}g\mu_B B_z \sigma_z + \frac{1}{2}g\mu_B \mathbf{B}(t) \cdot \boldsymbol{\sigma}. \quad (12)$$

As a result, rotation operators (Eq. 7) are defined as:

$$R_X(\theta; \lambda_x, \tau_{G_x}) = \exp\left(-i\sigma_x \frac{\theta(\lambda_x, \tau_{G_x})}{2}\right) \quad (13)$$

$$R_Y(\theta; \lambda_y, \tau_{G_y}) = \exp\left(-i\sigma_y \frac{\theta(\lambda_y, \tau_{G_y})}{2}\right) \quad (14)$$

$$R_Z(\theta; \lambda_z, \tau_{G_z}) = \exp\left(-i\sigma_z \frac{\theta(\lambda_z, \tau_{G_z})}{2}\right), \quad (15)$$

where $\lambda_i = \frac{1}{2}g\mu_B B_i, \forall i \in \{x, y, z\}$ is the energy associated with the interaction and $\theta(\lambda_i, \tau_{G_i}) = \lambda_i \tau_{G_i}$ is the rotation angle. Importantly, the rotation angle θ done depends on the gate time, τ_G and the value of λ_i .

Furthermore, the exchange interaction between electrons located in different QDs allows to perform multi-qubit (entangling) gates. The coupling can be controlled by means of the *voltage* detuning between their respective potentials [24]. Specifically, the exchange interaction Hamiltonian \mathbf{H}_{exc} is given by:

$$\mathbf{H}_{\text{exc}}(t) = \pm J_{\text{exc}}[\boldsymbol{\varepsilon}(t)] \mathbf{s}_1 \cdot \mathbf{s}_2, \quad (16)$$

where vector \mathbf{s}_i contains the spin operators of the electron in the i^{th} QD and $\pm J_{\text{exc}}[\boldsymbol{\varepsilon}(t)]$ is the exchange coupling strength between them. It depends on the voltage detuning, defined as $\boldsymbol{\varepsilon} = V_{\text{Ext}_1} - V_{\text{Ext}_2}$, where V_{Ext_i} is the potential applied to the i^{th} QD and its sign is a function of the magnetic properties of the semiconductor: ferromagnetic or antiferromagnetic. For the present manuscript, we will assume positive sign for $J_{\text{exc}}[\boldsymbol{\varepsilon}(t)]$ since the study is independent of its value, see Appendix B. Consequently, the total Hamiltonian to perform entangling gates is

$$\mathbf{H}_C(t) = \mathbf{H}_{\text{exc}}(t) + \sum_{j=1,2} \mathbf{H}_{Z,j}(t) \quad (17)$$

$$= J_{\text{exc}}[\boldsymbol{\varepsilon}(t)] \mathbf{s}_1 \cdot \mathbf{s}_2 + \sum_{i=1,2} g_i \mu_B \mathbf{B}(r_i, t) \cdot \mathbf{s}_i, \quad (18)$$

where $\mathbf{B}_i(r_i, t)$ is the magnetic field in the position of the i^{th} QD.

Finally, qubit readout is realized by means of the so-called spin-to-charge connection technique [25].

B. Spin Qubits in Double Quantum Dots

Spin qubits in QD infrastructures can be encoded in DQD systems with two electrons. Although two QDs are needed to encode a single qubit, this approach is advantageous because it can be resilient to certain sources of decoherence, such as hyperfine noise, because the $\text{SU}(2) \otimes \text{SU}(2)$ Hilbert space has a subspace without spin angular momentum in \hat{z} , see Appendix B. As a result, these systems exhibit longer coherence times, T_1 and T_2 [26]. The eigenstates of a system formed by 2 electrons are the singlet $|S\rangle$ and the triplet states ($|T_0\rangle$ and $|T_{\pm}\rangle$), which belong to the $\text{U}(1)$ and $\text{SU}(3)$ subspaces, respectively. Those states are defined as

$$|S\rangle = \frac{|\uparrow\downarrow\rangle - |\downarrow\uparrow\rangle}{\sqrt{2}}, \quad (19)$$

$$|T_+\rangle = |\uparrow\uparrow\rangle, \quad (20)$$

$$|T_0\rangle = \frac{|\uparrow\downarrow\rangle + |\downarrow\uparrow\rangle}{\sqrt{2}}, \quad (21)$$

$$|T_-\rangle = |\downarrow\downarrow\rangle. \quad (22)$$

The singlet state is anti-symmetric in its spin wave function and symmetric in its position wave function, allowing both electrons to occupy the same QD. In contrast, triplet states have a symmetric wave function in the spin basis and the electrons can not occupy the same QD due to Pauli exclusion principle. Along this document, we will study qubits encoded in a DQDs for the case that a single electron is loaded in each QD, i.e there is no hopping from one QD to the other. The interactions we are interested in are the exchange interaction, \mathbf{H}_{exc} (Eq. 16) and the Zeeman interaction, \mathbf{H}_Z (Eq. 10). Therefore, the Hamiltonian of a DQD system in the $\{|S\rangle, |T_0\rangle, |T_+\rangle, |T_-\rangle\}$ basis is given by:

$$\mathbf{H} = \mathbf{H}_Z + \mathbf{H}_{\text{exc}} = \begin{pmatrix} -\frac{1}{8}J_{\text{exc}}[\boldsymbol{\varepsilon}] & \frac{1}{2}g\mu_B \delta B_z & -\frac{1}{2\sqrt{2}}g\mu_B [\delta B_x + i\delta B_y] & \frac{1}{2\sqrt{2}}g\mu_B [\delta B_x - i\delta B_y] \\ \frac{1}{2}g\mu_B \delta B_z & \frac{1}{8}J_{\text{exc}}[\boldsymbol{\varepsilon}] & \frac{1}{2\sqrt{2}}g\mu_B [B_x + iB_y] & \frac{1}{2\sqrt{2}}g\mu_B [B_x - iB_y] \\ -\frac{1}{2\sqrt{2}}g\mu_B [\delta B_x - i\delta B_y] & \frac{1}{2\sqrt{2}}g\mu_B [B_x - iB_y] & \frac{1}{8}J_{\text{exc}}[\boldsymbol{\varepsilon}] + \frac{1}{2}g\mu_B B_z & 0 \\ \frac{1}{2\sqrt{2}}g\mu_B [\delta B_x + i\delta B_y] & \frac{1}{2\sqrt{2}}g\mu_B [B_x + iB_y] & 0 & \frac{1}{8}J_{\text{exc}}[\boldsymbol{\varepsilon}] - \frac{1}{2}g\mu_B B_z \end{pmatrix}, \quad (23)$$

where we have removed the explicit dependence on t on purpose to simplify the notation; $B_x = B_{x_1} + B_{x_2}$, $B_y = B_{y_1} + B_{y_2}$, $B_z = B_{z_1} + B_{z_2}$, $\delta B_x = (B_{x_1} - B_{x_2})$, $\delta B_y = (B_{y_1} - B_{y_2})$ and $\delta B_z = (B_{z_1} - B_{z_2})$. This Hamiltonian can be deduced from the Hamiltonian of the different interactions and from symmetry arguments (see Appendix A and B). There are different ways to encode a logical qubit in this system, such as ST_+ or flip-flop qubits (see Appendix C). In this work, we focus on ST_0 qubits, where the computational basis are formed by the states $|S\rangle \equiv |0\rangle$ and $|T_0\rangle \equiv |1\rangle$.

C. Singlet-Neutral triplet Qubits

The ST_0 qubit is encoded in the singlet $|S\rangle$ and neutral triplet $|T_0\rangle$ eigenstates of a DQD. To get this encoding, the Zeeman split of the energy levels should be $B_z \gg J_{\text{exc}}$ in order to make the energy gap between $|T_{\pm}\rangle$ states and the computational basis ($|S\rangle$ and $|T_0\rangle$) large enough. In this way, possible leakage from the computational subspace to the other accessible triplet states is reduced. We can write the effective Hamiltonian of the ST_0 from the Hamiltonian given in Eq. 23. The energy levels defining the encoded qubit are the states $|S\rangle$ and $|T_0\rangle$ given by the Hamiltonian H_{ST_0} :

$$H_{ST_0} = H_{\text{exc}} = \begin{pmatrix} \frac{J_{\text{exc}}[\varepsilon]}{8} & 0 \\ 0 & -\frac{J_{\text{exc}}[\varepsilon]}{8} \end{pmatrix} = \frac{J_{\text{exc}}[\varepsilon]}{8} \sigma_z, \quad (24)$$

where H_{exc} is the Heisenberg exchange Hamiltonian given in Eq. 16 with $\varepsilon(t) = \varepsilon$. To perform a rotation around the \hat{x} axis alone is not possible; instead, rotations around a combination of \hat{x} and \hat{z} axis are feasible. The Hamiltonian of the interaction between the qubit and an external magnetic field $\delta B_z(\mathbf{r}_1, \mathbf{r}_2) = B_z(\mathbf{r}_1, t) - B_z(\mathbf{r}_2, t)$ in the ST_0 subspace is:

$$H_Z(t) = g\mu_B \begin{pmatrix} 0 & \delta B_z(t)/2 \\ \delta B_z(t)/2 & 0 \end{pmatrix} = g\mu_B \frac{\delta B_z(t)}{2} \sigma_x. \quad (25)$$

Then, rotations around \hat{z} are achieved by manipulating the detuning to change the exchange coupling $J_{\text{exc}}[\varepsilon(t)]$ and around $\hat{x}\hat{z}$ by manipulating the external magnetic field δB_z . Respectively, the Hamiltonians are given by:

$$H_{R_z}(t) = \begin{pmatrix} J_{\text{exc}}[\varepsilon(t)]/8 & 0 \\ 0 & -J_{\text{exc}}[\varepsilon(t)]/8 \end{pmatrix} = \frac{J_{\text{exc}}[\varepsilon(t)]}{8} \sigma_z \quad (26)$$

$$\begin{aligned} H_{R_{xz}}(t) &= \frac{1}{2} g\mu_B \begin{pmatrix} \frac{J_{\text{exc}}[\varepsilon(t)]}{4g\mu_B} & \delta B_z(t) \\ \delta B_z(t) & -\frac{J_{\text{exc}}[\varepsilon(t)]}{4g\mu_B} \end{pmatrix} \\ &= g\mu_B \frac{\delta B_z(t)}{2} \sigma_x + \frac{J_{\text{exc}}[\varepsilon(t)]}{8} \sigma_z. \end{aligned} \quad (27)$$

Then the rotation operators are given by:

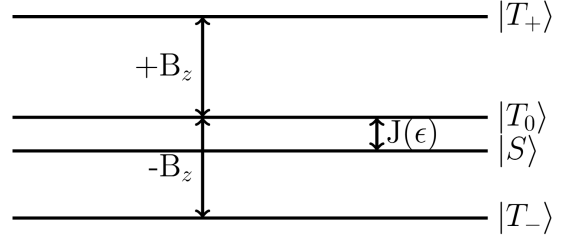


FIG. 2. Schematic representation of the energy levels of a DQD system with one electron in each QD. The Lie algebra is given by $SU(2) \otimes SU(2) = U(1) \oplus SU(3)$, i.e. the singlet and the triplets states. The Hamiltonian of the system is given in Eq.23 with $\mathbf{B} = (0, 0, B_z)$ and $\delta\mathbf{B} = (0, 0, 0)$

$$R(H(t), \tau_G) = \mathcal{T} \left\{ \exp \left(\frac{-i}{\hbar} \int_0^{\tau_G} dt H(t) \right) \right\} \quad (28)$$

$$= \exp \left(\frac{-i}{\hbar} \int_0^{\tau_G} dt g\mu_B \frac{\delta B_z(t)}{2} \sigma_x + \frac{J_{\text{exc}}[\varepsilon(t)]}{8} \sigma_z \right) \quad (29)$$

$$= \exp \left(\frac{-i}{\hbar} \left(g\mu_B \frac{\delta B_z}{2} \sigma_x + \frac{J_{\text{exc}}[\varepsilon]}{8} \sigma_z \right) \tau_G \right), \quad (30)$$

where $\mathcal{T}\{\cdot\}$ is the time ordering operator. Under the assumption of square pulses the Hamiltonian commuted with itself $[H(t_1), H(t_2)] = 0$ and $J_{\text{exc}}[\varepsilon(t)] = J_{\text{exc}}[\varepsilon]$ and $\delta B_z(t) = \delta B_z$ remain constants $\forall t_i \in [0, \tau_G]$. We define the angles as:

$$\theta_x = \tau_G \lambda_x = \tau_G g\mu_B \delta B_z, \quad (31)$$

$$\theta_z = \tau_G \lambda_z = \tau_G \frac{J_{\text{exc}}[\varepsilon]}{4}. \quad (32)$$

Then, the rotation operator is defined as:

$$R_{\hat{r}}(\theta_x + \theta_z) = \exp \left(\frac{-i}{\hbar} \frac{\theta_x \sigma_x + \theta_z \sigma_z}{2} \right), \quad (33)$$

where the rotation axis is:

$$\hat{r} = \frac{g\mu_B \frac{\delta B_z}{2} \hat{x} + \frac{J_{\text{exc}}[\varepsilon]}{8} \hat{z}}{\sqrt{\left(\frac{J_{\text{exc}}[\varepsilon]}{8} \right)^2 + \left(\frac{g\mu_B \delta B_z}{2} \right)^2}}. \quad (34)$$

These are the main interactions involving ST_0 qubits, any other rotation or entangling gate is formed by a combination of these interactions with different values of $J_{\text{exc};ij}[\varepsilon]$ and $\delta B_{z;ij}$ where i and j refer to different QDs [27].

III. TIME EVOLUTION OF ST_0 QUBITS

The goal now is to determine the free and controlled time evolution of an ST_0 qubit when there are transversal magnetic fields, i.e. $\mathbf{B}_{x,y}(\mathbf{r}, t) \neq 0$ and transitions between the computational basis and the $|T_{\pm}\rangle$ states are

TABLE I. These are the values of the different parameters and fields of the system used along the document. The values of the transversal fields B_x , δB_x , B_y and δB_y are not defined here because we change their value along the paper, since we want to observe their effect in the evolution.

Parameters	Values
g	2
m_e^{eff}	$0.9m_e^0 \frac{\text{eV}}{c^2}$
$\mu_B^{\text{eff}} = \frac{e\hbar}{2m_e^{\text{eff}}}$	$6.42915 \cdot 10^{-5} \left[\frac{\text{eV}}{\text{T}} \right]$
J_{exc}	2 [μeV]
B_z	100 [mT]
δB_z	10 [mT]

possible. In this scenario, the evolution of the system is described by the following Hamiltonian:

$$H = \begin{pmatrix} H_{ST_0} & H_{\text{leak}} \\ H_{\text{leak}}^\dagger & H_{T_\pm} \end{pmatrix}. \quad (35)$$

Instead of Eq. 26 and Eq. 27. The computational basis is given by the H_{ST_0} Hamiltonian given in Eq. 24. The $|T_\pm\rangle$ states are defined as (see Eq. 23):

$$H_{T_\pm} = \frac{1}{2}g\mu_B \begin{pmatrix} B_z + \frac{1}{4}J_{\text{exc}} & 0 \\ 0 & -B_z + \frac{1}{4}J_{\text{exc}} \end{pmatrix}. \quad (36)$$

Transitions from the computational basis to the T_\pm states are mediated by transversal fields $B_x(\mathbf{r})$ and $B_y(\mathbf{r})$ as:

$$H_{\text{leak}} = \frac{1}{2\sqrt{2}}g\mu_B \begin{pmatrix} -(\delta B_x + i\delta B_y) & \delta B_x - i\delta B_y \\ B_x + iB_y & B_x - iB_y \end{pmatrix}, \quad (37)$$

where again the dependence on t has been removed to simplify the notation. In absence of leakage terms, i.e. $H_{\text{leak}} = 0$, the computational basis ($|S\rangle$ and $|T_0\rangle$) are eigenstates, but in presence of transversal magnetic fields it is not the case. The eigenvalue of each eigenstate determines its evolution due to the Schrödinger equation. In presence of leakage, qubit rotations belongs to a 4-dimensional Hilbert space and the expression of a rotation using the generators of the space is more complex (See Appendix B). We use perturbation theory and a Dyson series expansion to study the dynamics of the system, i.e. to compare how the dynamics of the system change in presence of weak fields. In the next section, we analyze and compare the dynamics of the ST_0 qubit in different scenarios.

A. Simulations

In this section, we present a numerical analysis of the dynamics of the system. We refer to the population of a certain state $|\phi\rangle$ while evolving as $\text{Pop}(\phi, t)$. Assuming $|\psi(0)\rangle$ to be the initial state, the evolution of the previously mentioned population is given by:

$$\text{Pop}(\phi, t) = |\langle\phi|\psi(t)\rangle|^2. \quad (38)$$

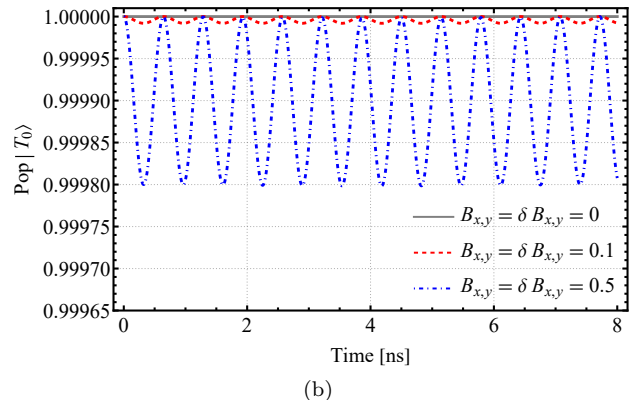
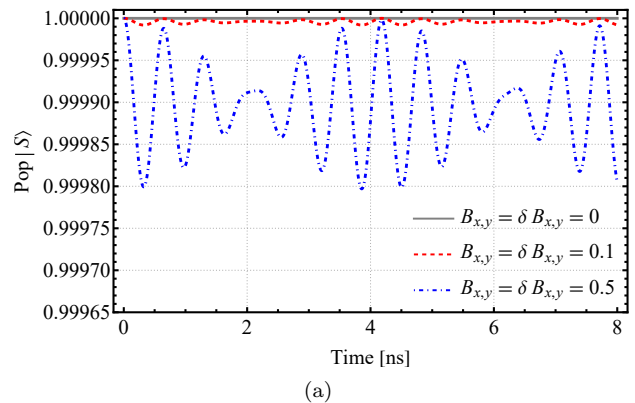


FIG. 3. Free evolution of (a) $|S\rangle$ and (b) $|T_0\rangle$ states in presence of leakage with $g = 2$, $\mu_B = 6.42915 \cdot 10^{-5} \left[\frac{\text{eV}}{\text{T}} \right]$, $B_z = 100$ [mT], $J_{\text{exc}} = 2$ [μeV]. We show three different cases: $B_{x,y} = \delta B_{x,y} = 0.1$ [mT] gray (solid) line, $B_{x,y} = \delta B_{x,y} = 0.1$ [mT] red (dashed) line and $B_{x,y} = \delta B_{x,y} = 0.5$ [mT] blue (dashed-dotted) line. We can observe that the population maintains constant when there is not magnetic transversal fields since the states are eigenstates of the Hamiltonian (Eq. 35), however in presence of them the population varies over time.

The dynamics is governed by the Hamiltonian given in Eq. 23. The values of the parameters we consider for the numerical simulations in this work are summarized in the Table I.

1. Free Evolution

The free evolution of the system is governed by the diagonal Hamiltonian Eq. 24. Without a transversal magnetic field, i.e. $\mathbf{B} = (0, 0, B_z)$, the singlet and triplet states are eigenstates of the Hamiltonian and their populations remain constant. Therefore, the Hamiltonian of the tetradimensional Hilbert space is defined as

$$\begin{aligned} H_{\text{Energy}} &= \frac{1}{8} J_{\text{exc}} \eta + \frac{1}{2} g \mu_B \left(\frac{B_z}{2} \Lambda_3 + \frac{\sqrt{3} B_z}{2} \Lambda_8 \right) \\ &= \frac{1}{2} g \mu_B \begin{pmatrix} -\frac{J_{\text{exc}}}{4g\mu_B} & 0 & 0 & 0 \\ 0 & \frac{J_{\text{exc}}}{4g\mu_B} & 0 & 0 \\ 0 & 0 & \frac{J_{\text{exc}}}{4g\mu_B} + B_z & 0 \\ 0 & 0 & 0 & \frac{J_{\text{exc}}}{4g\mu_B} - B_z \end{pmatrix}, \end{aligned} \quad (39)$$

where $\eta = \text{diag}(-1, +1, +1, +1)$, Λ_3 and Λ_8 are Gell-Mann matrices (See Appendix B); and we reorganized the terms to keep the order used in Eq. 35. The 4 eigenvalues are $\{\lambda_{|S\rangle} = -\frac{1}{8} J_{\text{exc}}, \lambda_{|T_0\rangle} = \frac{1}{8} J_{\text{exc}}, \lambda_{|T_+\rangle} = \frac{1}{8} J_{\text{exc}} + \frac{1}{2} g \mu_B B_z, \lambda_{|T_-\rangle} = \frac{1}{8} J_{\text{exc}} - \frac{1}{2} g \mu_B B_z\}$.

On the other hand, the singlet and triplet states are not eigenstates of the system when there is an external transversal field, so their populations will vary over time. The new eigenstates $\{\varphi_1, \varphi_2, \varphi_3, \varphi_4\}$ can be obtained by diagonalizing the new Hamiltonian and the singlet and triplet states can be represented as a linear combination of them:

$$\begin{aligned} |S\rangle &= \sum_i \alpha_i |\varphi_i\rangle, \\ |T_0\rangle &= \sum_i \beta_i |\varphi_i\rangle. \end{aligned} \quad (40)$$

In the same way, the $|T_{\pm}\rangle$ are represented as:

$$\begin{aligned} |T_+\rangle &= \sum_i \nu_i |\varphi_i\rangle, \\ |T_-\rangle &= \sum_i \kappa_i |\varphi_i\rangle. \end{aligned} \quad (41)$$

Each eigenstate has an associated eigenvalue $\{\lambda_1, \lambda_2, \lambda_3, \lambda_4\}$. Therefore, the time evolution operators are given by:

$$\begin{aligned} \hat{U}_{\varphi_1}(t_0, t) &= e^{-i\lambda_1(t-t_0)} |\varphi_1\rangle \langle \varphi_1|, \\ \hat{U}_{\varphi_2}(t_0, t) &= e^{-i\lambda_2(t-t_0)} |\varphi_2\rangle \langle \varphi_2|, \\ \hat{U}_{\varphi_3}(t_0, t) &= e^{-i\lambda_3(t-t_0)} |\varphi_3\rangle \langle \varphi_3|, \\ \hat{U}_{\varphi_4}(t_0, t) &= e^{-i\lambda_4(t-t_0)} |\varphi_4\rangle \langle \varphi_4|. \end{aligned}$$

Then, when we prepare an arbitrary state $|\psi\rangle = \xi_1 |\varphi_1\rangle + \xi_2 |\varphi_2\rangle + \xi_3 |\varphi_3\rangle + \xi_4 |\varphi_4\rangle$ and let it evolve over time, the temporal evolution of the population of certain state $|\zeta\rangle = a_1 |\varphi_1\rangle + a_2 |\varphi_2\rangle + a_3 |\varphi_3\rangle + a_4 |\varphi_4\rangle$ is given by:

$$\text{Pop}(\phi, t) = |\langle \zeta | \psi(t) \rangle|^2 \quad (42)$$

$$= |a_1^* \xi_1 e^{-i\lambda_1 t} + a_2^* \xi_2 e^{-i\lambda_2 t} \quad (43)$$

$$+ a_3^* \xi_3 e^{-i\lambda_3 t} + a_4^* \xi_4 e^{-i\lambda_4 t}|^2. \quad (44)$$

Using this equation we compute the evolution of the population of states $|S\rangle$ and $|T_0\rangle$ when the state is prepared as those, respectively, and for external transversal magnetic fields with magnitudes $B_{x,y} = \delta B_{x,y} = 0.1$ [mT]

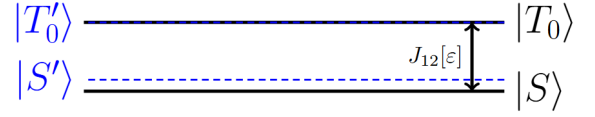


FIG. 4. Schematic representation of the computational states' energy shift due to transitions to higher energy levels using perturbation theory.

and $B_{x,y} = \delta B_{x,y} = 0.5$ [mT]. The results can be seen in Fig. 3. Panel (a) presents the population $|\langle S | S(t) \rangle|^2$, while panel (b) shows the population $|\langle T_0 | T_0(t) \rangle|^2$. For both of them, leakage to the T_{\pm} states occurs. At this stage, there is no external pulse inducing transitions of population between $|S\rangle$ and $|T_0\rangle$. However, the average population of the T_{\pm} states remains nonzero during the free evolution. This will influence the system's dynamics when we aim to apply rotations, as will be discussed in the following section.

2. Rotations

In the following, we analyze the dynamics of the ST₀ qubit when we apply external magnetic fields to induce single-qubit gates and, thus, study the impact of leakage on such rotations.

To perform rotations over different axes, we need to apply magnetic fields with different amplitudes and directions. Global magnetic fields do not break the $SU(2) \otimes SU(2)$ symmetry, By global we refer to the scenario in which the magnetic field is equal in both QDs. However, the components in the \hat{x} and/or \hat{y} of the external magnetic field break the spin angular momentum symmetry in direction \hat{z} (S_z) and allow transitions between levels with a difference in angular momentum ± 1 inside the $SU(3)$ subspace (recall that $SU(2) \otimes SU(2) = U(1) \oplus SU(3)$). Also, the $SU(2) \otimes SU(2)$ symmetry is broken when there exists a non-trivial gradient on the magnitudes of the external transversal magnetic fields, allowing transitions between the $U(1)$ and $SU(2)$ subspaces.

In this section, we continue assuming a constant value of the fields during the gate time. The Hamiltonian defining the singlet-triplet states (Eq. 39) and the time dependent rotation Hamiltonian depend on the values of the QD's potentials and the external magnetic fields. The dynamics is then defined by the following Hamiltonian:

$$H_{\text{Gate}} = H_{\text{Energy}} + H_R(t), \quad (45)$$

where $H_R(t)$ is defined by the Hamiltonian given in Eq. 23. First, we will study rotations around the \hat{z} axis induced by applying an external electric field that changes the exchange coupling, J_{exc} . Such rotations change the relative phase between the states $|S\rangle$ and $|T_0\rangle$, but do not induce transitions between them. Given a general state $|\psi\rangle = \alpha |S\rangle + \beta |T_0\rangle$, the relative phase change over time is

TABLE II. In this table we show the dependence of the energies of the eigenstates on the values of the transversal magnetic field. We have chosen the values $J_{\text{exc}} = 2$ [μeV] and $B_z = 100$ [mT]. We differentiate three different cases for the magnetic field: $B_{x,y} = \delta B_{x,y} = 0.1$ [mT], $B_{x,y} = \delta B_{x,y} = 0.1$ [mT] and $B_{x,y} = \delta B_{x,y} = 0.5$ [mT].

State	$B_{x,y} = 0$	$B_{x,y} = \delta B_{x,y} = 0.1$	$B_{x,y} = \delta B_{x,y} = 0.5$
λ'_1	$-2.5 \cdot 10^{-7}$	$-2.49999 \cdot 10^{-7}$	$-2.49975 \cdot 10^{-7}$
λ'_2	$2.5 \cdot 10^{-7}$	$2.5 \cdot 10^{-7}$	$2.5 \cdot 10^{-7}$
λ'_3	$6.67915 \cdot 10^{-6}$	$6.67916 \cdot 10^{-6}$	$6.67946 \cdot 10^{-6}$
λ'_4	$-6.17915 \cdot 10^{-6}$	$-6.17917 \cdot 10^{-6}$	$-6.17949 \cdot 10^{-6}$

given by:

$$\begin{aligned}
|\psi(t)\rangle &= \alpha \hat{U}_{\lambda_1}(0,t) |S\rangle + \beta \hat{U}_{\lambda_2}(0,t) |T_0\rangle \\
&= \hat{U}_{\lambda_1} \left(\alpha |S\rangle + \beta \frac{\hat{U}_{\lambda_2}(0,t)}{\hat{U}_{\lambda_1}(0,t)} |T_0\rangle \right) \\
&= \alpha |S\rangle + \beta e^{\frac{-i}{\hbar}(\lambda_{|T_0\rangle} - \lambda_{|S\rangle})t} |T_0\rangle, \quad (46)
\end{aligned}$$

where $\lambda_{|S\rangle} = -\frac{1}{8}J_{\text{exc}}$ and $\lambda_{|T_0\rangle} = \frac{1}{8}J_{\text{exc}}$ are the eigenvalues of the Hamiltonian. Note that the value of J_{exc} changes during the gate time τ_G due to the variation of ε . As we stated before, when there is an external transversal magnetic field that may induce leakage, we can express the singlet-triplet states as a linear combination of the new eigenstates of the Hamiltonian $\{\phi_1, \phi_2, \phi_3, \phi_4\}$:

$$|S\rangle = \sum_i \alpha'_i |\phi_i\rangle, \quad (47)$$

$$|T_0\rangle = \sum_i \beta'_i |\phi_i\rangle, \quad (48)$$

$$|T_+\rangle = \sum_i \nu'_i |\phi_i\rangle, \quad (49)$$

$$|T_-\rangle = \sum_i \kappa'_i |\phi_i\rangle, \quad (50)$$

where $\alpha'_i, \beta'_i, \nu'_i, \kappa'_i$ are complex amplitudes and the new eigenvalues are $\{\lambda'_1, \lambda'_2, \lambda'_3, \lambda'_4\}$.

To mathematically analyze how leakage changes the dynamics, we use perturbation theory (PT) since we are working in the weak transversal field regime, i.e. $|\pm \frac{1}{2\sqrt{2}}g\mu_B(\delta B_x \pm i\delta B_y)|, |\pm \frac{1}{2\sqrt{2}}g\mu_B(B_x \pm iB_y)| \ll |\frac{J_{\text{exc}}}{8}|$. We can split the Hamiltonian in two different parts: The unperturbed Hamiltonian

H_0 given in Eq. 39, and the perturbed Hamiltonian H_p formed by the non-diagonal terms. Then, the new eigenvalues can be approximated as:

$$\lambda'_1 \approx \lambda_1 + \sum_m \frac{\langle S|H_I|m\rangle \langle m|H_I|S\rangle}{\lambda_1 - \lambda_m}, \quad (51)$$

$$\lambda'_2 \approx \lambda_2 + \sum_m \frac{\langle T_0|H_I|m\rangle \langle m|H_I|T_0\rangle}{\lambda_2 - \lambda_m}, \quad (52)$$

$$\lambda'_3 \approx \lambda_3 + \sum_m \frac{\langle T_+|H_I|m\rangle \langle m|H_I|T_+\rangle}{\lambda_3 - \lambda_m}, \quad (53)$$

$$\lambda'_4 \approx \lambda_4 + \sum_m \frac{\langle T_-|H_I|m\rangle \langle m|H_I|T_-\rangle}{\lambda_4 - \lambda_m}. \quad (54)$$

In theory, the perturbation could make the energy gap between λ_1 and λ_2 larger or smaller, but for the DQD system it only reduces the value of λ_1 . The shift of the eigenvalues of the computational states is represented graphically in Fig. 4.

Now, given an arbitrary state $|\psi\rangle = \alpha|\phi_1\rangle + \beta|\phi_2\rangle$, it will evolve as (see Eq. 46):

$$|\psi(t)\rangle = \alpha|\phi_1\rangle + \beta e^{\frac{-i}{\hbar}(\lambda'_2 - \lambda'_1)t} |\phi_2\rangle. \quad (55)$$

Then, the time to perform the desired relative phase change for the computational basis depends not only on the values of J_{exc} , but also on the values of the transverse magnetic field. If $(\lambda'_2 - \lambda'_1) > (\lambda_{|T_0\rangle} - \lambda_{|S\rangle})$ for a given external magnetic field \mathbf{B} , the time required to perform a rotation would decrease, and viceversa. However, in the case of a small perturbation, the eigenvalue λ'_2 will remain unchanged while eigenvalue λ'_1 will be always larger than $\lambda_{|S\rangle}$, thus, $(\lambda'_2 - \lambda'_1) \leq (\lambda_{|T_0\rangle} - \lambda_{|S\rangle})$ for any amplitude of the external transversal magnetic fields. We compute the eigenvalues of the Hamiltonian for different external magnetic fields in this regime, which are given in Tab. II. The evolution of the state $|+\rangle = \frac{|S\rangle + |T_0\rangle}{\sqrt{2}}$ during the rotation is shown in the panel a of the Fig. 5 for different values of the transversal magnetic fields. We observe that the rotation in presence of leakage terms is slower than the rotation without them, i.e. there is a phase change between both evolutions due to the shift in the energies. This phase change grows when the amplitudes of the transversal magnetic fields increase or when the energy gap between the states $|T_{\pm}\rangle$ and the computational states is reduced.

To perform rotations around the \hat{x} axis, we have to vary the external magnetic field in the \hat{z} direction to create a non-trivial magnetic field gradient between the QDs, i.e. $\delta B_z \neq 0$. Now, the situation is completely different because this field is not in the weak regime and we cannot use PT to study the effect of leakage on the dynamics. In the case of ST₀ qubits without leakage, a rotation was defined in Eq. 33; which in the presence of leakage is given by:

$$\begin{aligned}
R(H, \tau_g) &= \mathcal{T} \left\{ \exp \left(\frac{-i}{2} \int_0^{\tau_g} dt \left[\frac{1}{8} J_{\text{exc}} \eta + \frac{1}{2} g\mu_B \left(\frac{B_z}{2} \Lambda_3 + \frac{\sqrt{3}B_z}{2} \Lambda_8 + \frac{1}{\sqrt{2}} B_x \Lambda_1 + \frac{1}{\sqrt{2}} B_x \Lambda_6 + \frac{1}{\sqrt{2}} B_y \Lambda_2 + \frac{1}{\sqrt{2}} B_y \Lambda_7 \right) \right. \right. \right. \\
&\quad \left. \left. \left. + \frac{1}{2} g\mu_b (\delta B_z \Lambda'_3 - \frac{1}{\sqrt{2}} \delta B_x \Lambda'_1 + \frac{1}{\sqrt{2}} \delta B_x \Lambda'_3 + \frac{1}{\sqrt{2}} \delta B_y \Lambda'_2 + \frac{1}{\sqrt{2}} \delta B_y \Lambda'_6) \right] \right) \right\}, \quad (56)
\end{aligned}$$

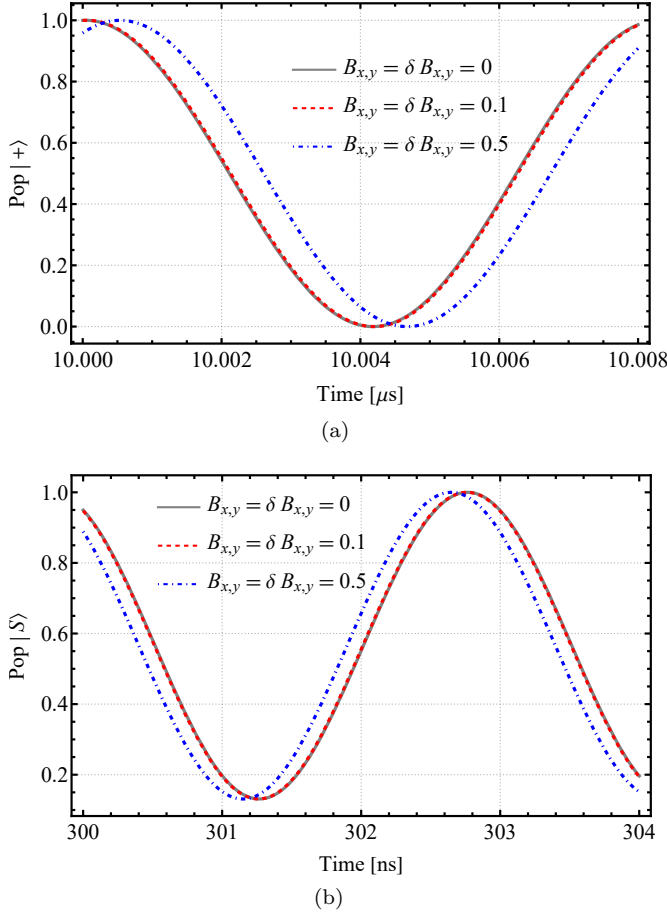


FIG. 5. Time evolution of the population of the state (a) $|+\rangle$ for a rotation around the \hat{z} direction when the initial state is $|+\rangle$ at $t=0$ and (b) $|S\rangle$ for a rotation around the $\hat{x}\hat{z}$ axis when the initial state is $|S\rangle$ at $t=0$. We compare the evolution when there are not and when there are transversal fields with values: $B_{x,y} = \delta B_{x,y} = 0.1$ mT and $B_{x,y} = \delta B_{x,y} = 0.5$ mT. We allowed the system to evolve so that the dephasing is noticeable and zoomed in to such time scale.

where Λ_i are the Gell-mann matrices and Λ'_i are rotations that break the $SU(2) \otimes SU(2)$ symmetry. This equation is explained and deduced in Appendix B.

We study the rotations induced by the Hamiltonian using the time ordering operator and expand it using a Dyson series (see Appendix D). We get the evolution operators for transitions $|S\rangle \rightarrow |T_0\rangle$ and $|T_0\rangle \rightarrow |S\rangle$, which are given by the same expression since $\langle S|H_I(t)|T_0\rangle = \left(\langle T_0|H_I^\dagger(t)|S\rangle\right)^\dagger = \left(\langle T_0|H_I(t)|S\rangle\right)^\dagger$, using the hermitian property of the Hamiltonian $H = H^\dagger$. To work with the Dyson series we split the Hamiltonian in its non-interacting or diagonal terms given in Eq. 39 and in its interacting or off-diagonal terms:

$$H_I(t) = \begin{pmatrix} 0 & \\ & H_{I\{T_0, T_\pm\}} \end{pmatrix} + H_{I\{BS\}}, \quad (57)$$

where:

$$H_{I\{T_0, T_\pm\}} = \frac{1}{2}g\mu_B \begin{pmatrix} 0 & \frac{1}{\sqrt{2}}(B_x - iB_y) & 0 \\ \frac{1}{\sqrt{2}}(B_x + iB_y) & 0 & \frac{1}{\sqrt{2}}(B_x - iB_y) \\ 0 & \frac{1}{\sqrt{2}}(B_x + iB_y) & 0 \end{pmatrix}, \quad (58)$$

and

$$H_{I\{BS\}} = \frac{1}{2}g\mu_b \begin{pmatrix} 0 & \frac{-1}{\sqrt{2}}(\delta B_x + i\delta B_y) & \delta B_z & \frac{1}{\sqrt{2}}(\delta B_x - i\delta B_y) \\ \frac{-1}{\sqrt{2}}(\delta B_x - i\delta B_y) & 0 & 0 & 0 \\ \delta B_z & 0 & 0 & 0 \\ \frac{1}{\sqrt{2}}(\delta B_x + i\delta B_y) & 0 & 0 & 0 \end{pmatrix}. \quad (59)$$

Both expressions are deduced in Appendix B. The unitary evolution operator when only the term $\delta B_z \neq 0$ is given by:

$$\hat{U}_I(\tau_G, 0) = \exp\left(\frac{-i\tau_G}{\hbar} \frac{1}{2}g\mu_B \delta B_z \sigma_x\right). \quad (60)$$

However, whenever we apply a general magnetic field, using Eq. 56 and a Dyson series, we can rewrite approximately the unitary evolution of a rotation around \hat{x} as:

$$\hat{U}_I(t, 0) \approx \frac{-it}{\hbar} \frac{1}{2}g\mu_B \delta B_z \quad (61)$$

$$-i\left(\frac{t}{\hbar}\right)^2 \left(\frac{1}{2\sqrt{2}}g\mu_B\right)^2 (\delta B_x B_y - \delta B_y B_x) \quad (62)$$

The phase change between the time evolution of the system with and without leakage is given by the difference in the argument of the unitary operators in Eq. 60 and in Eq. 61. Furthermore, we can compute the effective amplitudes of the transitions at second order approximation as:

$$A_{|S\rangle \rightarrow |T_0\rangle} = \frac{1}{2}g\mu_B \delta B_z \quad (63)$$

$$+ \frac{\left(\frac{1}{2}g\mu_B\right)^2 (B_x - iB_y) (\delta B_x + i\delta B_y)}{E_{|S\rangle} - E_{|T_-\rangle}} \quad (64)$$

$$+ \frac{\left(\frac{1}{2}g\mu_B\right)^2 (B_x + iB_y) (\delta B_x - i\delta B_y)}{E_{|S\rangle} - E_{|T_+\rangle}} \quad (65)$$

and

$$A_{|T_0\rangle \rightarrow |S\rangle} = \frac{1}{2}g\mu_B \delta B_z \quad (66)$$

$$+ \frac{\left(\frac{1}{2}g\mu_B\right)^2 (B_x + iB_y) (\delta B_x - i\delta B_y)}{E_{|T_0\rangle} - E_{|T_-\rangle}} \quad (67)$$

$$+ \frac{\left(\frac{1}{2}g\mu_B\right)^2 (B_x - iB_y) (\delta B_x + i\delta B_y)}{E_{|T_0\rangle} - E_{|T_+\rangle}}. \quad (68)$$

The evolution of the state $|S\rangle$ during the rotation is shown in the panel a of the Fig. 5 for different values of the transversal magnetic fields. Now, we can write the effective Hamiltonian of the dynamics of the ST_0 qubit as:

$$H_{\text{eff}}(t) = \begin{pmatrix} \lambda'_1 & A_{|T_0\rangle \rightarrow |S\rangle} \\ A_{|S\rangle \rightarrow |T_0\rangle} & \lambda'_2 \end{pmatrix}, \quad (69)$$

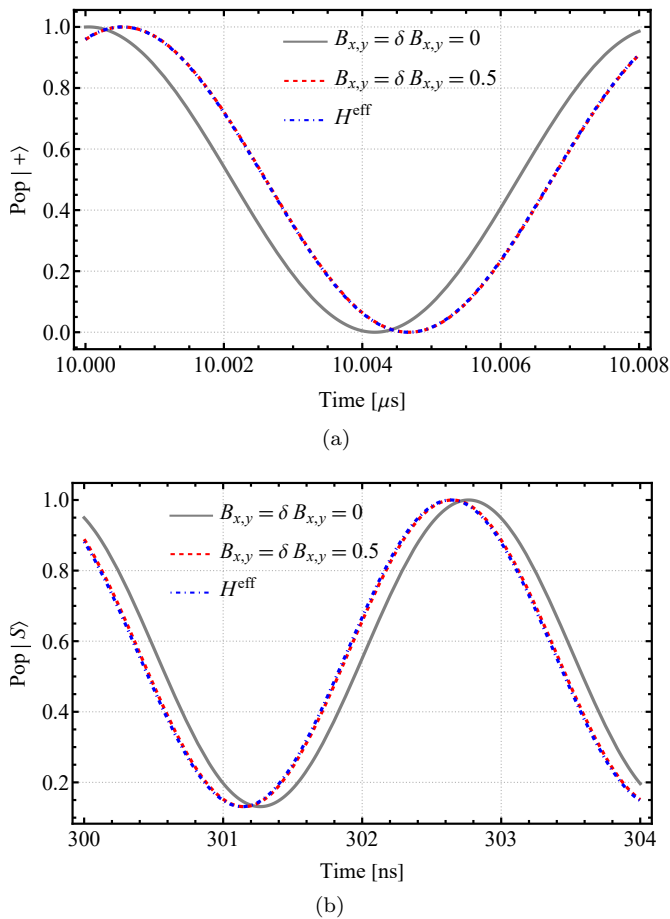


FIG. 6. Comparison of the time evolution of the states $|+\rangle$ (a) when a rotation around \hat{z} is performed and $|S\rangle$ (b) when we apply a magnetic field such as $\delta B_z = 10$ [mT]. We allowed the system to evolve so that the dephasing is noticeable and zoomed in to such time scale. We have The gray (solid) line is the evolution without leakage terms, the red (dashed) line is the evolution with leakage by solving Eq. 56 and the blue (dashed-dotted) by solving Eq.33 using the effective Hamiltonian given in Eq. 69. The transversal magnetic field is $B_{x,y} = \delta B_{x,y} = 0.5$ [mT]. We allowed the system to evolve so that the dephasing is noticeable and zoomed in to such time scale.

where λ'_1 and λ'_2 are given in Eq. 51 and Eq. 52, respectively. Finally, we can compute the rotation operators as $R(H_{\text{eff}}(t), \tau_g)$ using Eq. 30 instead of resolving the rotation in the Hilbert space of dimension 4 given in Eq. 56. In Fig. 6, we compare the evolution of the system without leakage with the evolution defined by the Hamiltonian with transversal magnetic fields by solving the rotation given in Eq. 56 and by solving the rotation given in Eq. 33 with the effective Hamiltonian given in Eq. 69, respectively. The evolution defined by the effective Hamiltonian is a good approximation to the actual evolution. Furthermore, it gives us the freedom to control the speed of the time evolution operators by means of the signs and amplitudes of the transversal magnetic fields.

IV. DISCUSSION

Encoding qubits in the singlet-triplet states in DQD devices is an interesting approach since the spin angular momentum in direction \hat{z} of those states is zero implying resilience against hyperfine noise in the surrounding. Furthermore, one can theoretically isolate the $|S\rangle$ and $|T_0\rangle$ states to avoid transitions to other states such as $|T_{\pm}\rangle$. However, this is not experimentally easy since on an actual semiconductor heterostructure different sources of noise that break the L_z and the spin-position symmetry exist, such as hyperfine and spin-orbit interactions [1]. Noise reduces the coherence time of the state encoded in a qubit and results in erroneous results obtained after running a quantum algorithm.

Since leakage usually comes from interactions with the environment, it contributes to incoherent errors and it is studied as a source of decoherence of the quantum state [16]. However, we discussed that leakage has an impact on the dynamics of the system, causing a shift in the quantum evolution operator and, hence, over or under rotations. We studied it under the assumption of constant pulses during the gate time, which is not far from the actual pulses implemented experimentally [28]. As shown, leakage produces faster (or slower) rotations depending on the amplitude of the interaction and the energy gap between the computational basis and the other accessible states. To implement such transitions artificially, we have to apply magnetic fields to a set of QDs. However, it is not generally easy to apply and control the magnetic fields in all directions and positions of the device [29, 30]. In this paper, we studied the ideal evolution of the ST_0 spin qubits in DQD devices in the presence of leakage. Our analysis is agnostic on the source of the interactions producing the leakage since they might come from the environment and/or from the applications of external fields. Furthermore, while in this work we have studied single qubit gates, entangling gates between pairs of singlet-triplet qubits encoded in DQDs are realized by means of similar pulses, i.e. based on transverse magnetic fields and exchange interaction, and, thus, we expect similar results for those[27].

Quantum algorithms require the application of a huge amount of very calibrated rotations over large amounts of qubits. For example, more than 10^{18} gates are needed for running Shor's algorithm in a fault-tolerant manner [31]. In this sense, although the time required to perform a single rotation is very short (on the order of nanoseconds), the coherence time of spin qubits is also quite limited: T_1 is on the order of milliseconds, and T_2 on the order of tens of microseconds. Furthermore, these values depend on the specific technology and experimental setup [1]. Therefore, the obtained results are not even a good approximation of the true value due to decoherence. We showed that having control over the external magnetic fields gives the possibility to reduce the required time to perform certain rotations. Even a very small reduction of the required time to perform a rotation would have an important impact in the time needed to run a long quantum algorithm. Also, shorter gate times result in less exposure to decoherence processes.

Additionally, in the paradigm of QEC is very important to characterize all the different possible noise sources so that they can effectively be treated. The code threshold refers to the physical error rate below which certain QEC code effectively reduces the probability of logical errors for certain noise model [32–34]. To compute this value a characterization of

the different sources of noise is needed. Leakage is usually considered as a probability the measuring a qubit on a state outside the computational basis and, thus, can be treated as an erasure errors [16]. Nevertheless, as we discuss in this work, it is also a source of gate errors due to over- or under-rotations which influences a QEC process or a quantum algorithm. Coherent errors can be made into stochastic errors by means of Pauli twirling, so leakage could contribute by increasing the gate physical error rate as discussed in this work [5].

In contrast, QEM techniques try to reduce the noise during the execution of a quantum algorithm using classical post-processing algorithms [7]. In the NISQ era, QEM is a promising post-processing technique to improve the precision of current quantum computers until fault-tolerant quantum computers are constructed. Many different QEM techniques exist, all of which require a good characterization of the noise. For example, ZNE the existence of a tunable global noise source, i.e. a way to control all the noise rates of a system globally [8]. Usually, such global noise source can be obtained by controlling the time needed to run the algorithm, i.e. changing the time needed to perform each rotation. This noise amplification technique is referred to as pulse stretching [35, 36]. In this work, we discussed how controlling the leakage terms of the system allows to change the required time to perform a rotation and, hence, could be useful to tune the error rate of a quantum computer and to implement ZNE techniques.

V. CONCLUSION

Qubits are encoded in quantum systems which, generally, have more than two accessible levels. Usually, the implementation of a qubit in physical devices, such as QDs, is done in such a way that the probability of leakage out of the computational subspace is very low. The main reason is to reduce the decoherence suffered by the system due to these transitions. However, reducing those to zero is generally impossible, implying the emergence of leakage errors. In this work, we discussed how leakage has an impact on the evolution of the system when an external field to perform a rotation is applied, producing over- or under-rotations. The change of the quantum evolution operator depends on the amplitudes of the interactions, the desired rotation and the energy gap between the energy levels of the system. Even if the difference is small, coherent errors accumulate for deep circuits resulting in ultimate failure. This result is important to understand the evolution of systems with more than two accessible levels with transitions among them induced by means of noise or

gate control. In addition to this result, we showed that having control over the leakage terms allows to change the time required to perform a rotation, which could be used to vary a tunable global noise source to implement ZNE techniques.

In this sense, an interesting follow up to this work would be to analyze what happens to the system dynamics when noise is present, e.g. Markovian relaxation or dephasing channels. In this work, we decoupled the evolution from this effect in order to isolate what is the impact of leakage, but for a realistic system, all effects would occur at the same time. Thus, it would be interesting to see how the faster or slower evolution that leakage sometimes induces has an impact in the amount of noise of the system. This is mainly because a shorter evolution in principle should result in less noise, but at the same time, the leakage term can also imply a loss in fidelity. So a nice trade-off among those effects could be found by controlling the leakage terms as discussed here, resulting in optimized pulses for these systems. As mentioned before, this can also be useful to realize ZNE like error mitigation techniques over singlet-triplet qubits encoded in DQDs or other quantum devices with more than 2 accessible levels.

In addition, experimentally verifying the conclusions obtained would be important to confirm these results. As mentioned, we assume pulses that are easily implementable in experiment, so implementing experiments would not require exotic pulse generators. The most challenging part would probably be the use of transversal magnetic fields that tune the leakage terms, but we consider that this can be handled. As a result, a better understanding of the effect of leakage on the evolution of quantum systems would be obtained, which is critical to make practical quantum computations.

ACKNOWLEDGEMENTS

We thank other members of the Hitachi-Cambridge Laboratory and the Quantum Information Group at Tecnun for their support and many useful discussions. This work was partially supported by the Spanish Ministry of Science and Innovation through the project ‘‘Few-qubit quantum hardware, algorithms and codes, on photonic and solidstate systems’’ (PLEC2021-008251) and by the Diputaci3n Foral de Gipuzkoa through the ‘‘Biased quantum error mitigation and applications of quantum computing to gene regulatory networks’’ project (2024-QUAN-000020). J.E.M. is funded by the Spanish Ministry of Science, Innovation and Universities through a Jose Castillejo mobility grant for his stay at the Cavendish Laboratory of the University of Cambridge.

-
- [1] G. Burkard, T. D. Ladd, A. Pan, J. M. Nichol, and J. R. Petta, ‘‘Semiconductor spin qubits,’’ *Rev. Mod. Phys.*, 2023.
- [2] T. Fujisawa, D. G. Austing, Y. Hirayama, and S. Tarucha, ‘‘Electrical pump and probe measurements of a quantum dot in the coulomb blockade regime,’’ *Japanese Journal of Applied Physics*, vol. 42, no. 7S, p. 4804, jul 2003. [Online]. Available: <https://dx.doi.org/10.1143/JJAP.42.4804>
- [3] K. Saeedi, S. Simmons, J. Z. Salvail, P. Dluhy, H. Riemann, N. V. Abrosimov, P. Becker, H.-J. Pohl, J. J. L. Morton, and M. L. W. Thewalt, ‘‘Room-temperature quantum bit storage exceeding 39 minutes using ionized donors in silicon-28,’’ *Science*, vol. 342, no. 6160, pp. 830–833, 2013. [Online]. Available: <https://www.science.org/doi/abs/10.1126/science.1239584>
- [4] Z. Cai, X. Xu, and S. C. Benjamin, ‘‘Mitigating coherent noise using pauli conjugation,’’ *npj Quantum Information*, vol. 6, no. 1, p. 17, Feb 2020. [Online]. Available: <https://doi.org/10.1038/s41534-019-0233-0>
- [5] A. deMartı iOlius, P. Fuentes, R. Orús, P. M. Crespo, and J. Etxezarreta Martinez, ‘‘Decoding

- algorithms for surface codes,” *Quantum*, vol. 8, p. 1498, Oct. 2024. [Online]. Available: <https://doi.org/10.22331/q-2024-10-10-1498>
- [6] Z. Cai, R. Babbush, S. C. Benjamin, S. Endo, W. J. Huggins, Y. Li, J. R. McClean, and T. E. O’Brien, “Quantum error mitigation,” *Rev. Mod. Phys.*, vol. 95, p. 045005, Dec 2023. [Online]. Available: <https://link.aps.org/doi/10.1103/RevModPhys.95.045005>
- [7] K. Temme, S. Bravyi, and J. M. Gambetta, “Error mitigation for short-depth quantum circuits,” *Phys. Rev. Lett.*, vol. 119, p. 180509, Nov 2017. [Online]. Available: <https://link.aps.org/doi/10.1103/PhysRevLett.119.180509>
- [8] J. Etxezarreta Martinez, O. Sanz Larrarte, J. Oliva del Moral, R. Dastbasteh, and R. M. Otxoa, “Comment on “recovering noise-free quantum observables”,” *Phys. Rev. A*, vol. 110, p. 046401, Oct 2024. [Online]. Available: <https://link.aps.org/doi/10.1103/PhysRevA.110.046401>
- [9] Google Quantum AI, “Quantum error correction below the surface code threshold,” *arXiv e-prints*, p. arXiv:2408.13687, Aug. 2024.
- [10] E. T. Campbell, B. M. Terhal, and C. Vuillot, “Roads towards fault-tolerant universal quantum computation,” *Nature*, vol. 549, no. 7671, pp. 172–179, Sep 2017. [Online]. Available: <https://doi.org/10.1038/nature23460>
- [11] D. Gottesman, “An introduction to quantum error correction and fault-tolerant quantum computation,” 2009. [Online]. Available: <https://arxiv.org/abs/0904.2557>
- [12] M.-Y. Chen, C. Zhang, and Z.-Y. Xue, “Fast high-fidelity geometric gates for singlet-triplet qubits,” *Phys. Rev. A*, vol. 105, p. 022620, Feb 2022. [Online]. Available: <https://link.aps.org/doi/10.1103/PhysRevA.105.022620>
- [13] A. Asthana, C. Liu, O. R. Meitei, S. E. Economou, E. Barnes, and N. J. Mayhall, “Leakage reduces device coherence demands for pulse-level molecular simulations,” *Physical Review Applied*, vol. 10, p. 64071, 2023.
- [14] K. C. Miao, M. McEwen, J. Atalaya, D. Kafri, L. P. Pryadko, A. Bengtsson, A. Opremcak, K. J. Satzinger, Z. Chen, P. V. Klimov, C. Quintana, R. Acharya, K. Anderson, M. Ansmann, F. Arute, K. Arya, A. Asfaw, J. C. Bardin, A. Bourassa, J. Bovaird, L. Brill, B. B. Buckley, D. A. Buell, T. Burger, B. Burkett, N. Bushnell, J. Campero, B. Chiaro, R. Collins, P. Conner, A. L. Crook, B. Curtin, D. M. Debroy, S. Demura, A. Dunsworth, C. Erickson, R. Fatemi, V. S. Ferreira, L. F. Burgos, E. Forati, A. G. Fowler, B. Foxen, G. Garcia, W. Giang, C. Gidney, M. Giustina, R. Gosula, A. G. Dau, J. A. Gross, M. C. Hamilton, S. D. Harrington, P. Heu, J. Hilton, M. R. Hoffmann, S. Hong, T. Huang, A. Huff, J. Iveland, E. Jeffrey, Z. Jiang, C. Jones, J. Kelly, S. Kim, F. Kostritsa, J. M. Kreikebaum, D. Landhuis, P. Laptev, L. Laws, K. Lee, B. J. Lester, A. T. Lill, W. Liu, A. Locharla, E. Lucero, S. Martin, A. Megrant, X. Mi, S. Montazeri, A. Morvan, O. Naaman, M. Neeley, C. Neill, A. Nersisyan, M. Newman, J. H. Ng, A. Nguyen, M. Nguyen, R. Potter, C. Rocque, P. Roushan, K. Sankaragomathi, H. F. Schurkus, C. Schuster, M. J. Shearn, A. Shorter, N. Shutty, V. Shvarts, J. Skrzynny, W. C. Smith, G. Sterling, M. Szalay, D. Thor, A. Torres, T. White, B. W. K. Woo, Z. J. Yao, P. Yeh, J. Yoo, G. Young, A. Zalcman, N. Zhu, N. Zobrist, H. Neven, V. Smelyanskiy, A. Petukhov, A. N. Korotkov, D. Sank, and Y. Chen, “Overcoming leakage in quantum error correction,” *Nature Physics*, vol. 19, no. 12, pp. 1780–1786, Dec 2023. [Online]. Available: <https://doi.org/10.1038/s41567-023-02226-w>
- [15] Z. Cai, M. A. Fogarty, S. Schaal, S. Patomäki, S. C. Benjamin, and J. J. L. Morton, “A Silicon Surface Code Architecture Resilient Against Leakage Errors,” *Quantum*, vol. 3, p. 212, Dec. 2019. [Online]. Available: <https://doi.org/10.22331/q-2019-12-09-212>
- [16] C. J. Wood and J. M. Gambetta, “Quantification and characterization of leakage errors,” *Phys. Rev. A*, vol. 97, p. 032306, Mar 2018. [Online]. Available: <https://link.aps.org/doi/10.1103/PhysRevA.97.032306>
- [17] G. Schedelbeck, W. Wegscheider, M. Bichler, and G. Abstreiter, “Coupled quantum dots fabricated by cleaved edge overgrowth: From artificial atoms to molecules,” *Science*, vol. 278, no. 5344, pp. 1792–1795, 1997. [Online]. Available: <https://www.science.org/doi/abs/10.1126/science.278.5344.1792>
- [18] L. Fedichkin, M. Yanchenko, and K. A. Valiev, “Coherent charge qubits based on gaas quantum dots with a built-in barrier,” *Nanotechnology*, vol. 11, no. 4, p. 387, dec 2000. [Online]. Available: <https://dx.doi.org/10.1088/0957-4484/11/4/339>
- [19] S.-S. Li, J.-B. Xia, J.-L. Liu, F.-H. Yang, Z.-C. Niu, S.-L. Feng, and H.-Z. Zheng, “Inas/gaas single-electron quantum dot qubit,” *Journal of Applied physics*, vol. 90, no. 12, pp. 6151–6155, 2001.
- [20] D. Culcer, L. Cywiński, Q. Li, X. Hu, and S. Das Sarma, “Quantum dot spin qubits in silicon: Multivalley physics,” *Phys. Rev. B*, vol. 82, p. 155312, Oct 2010. [Online]. Available: <https://link.aps.org/doi/10.1103/PhysRevB.82.155312>
- [21] F. A. Zwanenburg, A. S. Dzurak, A. Morello, M. Y. Simmons, L. C. L. Hollenberg, G. Klimeck, S. Rogge, S. N. Coppersmith, and M. A. Eriksson, “Silicon quantum electronics,” *Rev. Mod. Phys.*, vol. 85, pp. 961–1019, Jul 2013. [Online]. Available: <https://link.aps.org/doi/10.1103/RevModPhys.85.961>
- [22] J. J. L. Morton, D. R. McCamey, M. A. Eriksson, and S. A. Lyon, “Embracing the quantum limit in silicon computing,” *Nature*, vol. 479, no. 7373, p. 345–353, Nov. 2011. [Online]. Available: <http://dx.doi.org/10.1038/nature10681>
- [23] Y. Meir, N. S. Wingreen, and P. A. Lee, “Transport through a strongly interacting electron system: Theory of periodic conductance oscillations,” *Phys. Rev. Lett.*, vol. 66, pp. 3048–3051, Jun 1991. [Online]. Available: <https://link.aps.org/doi/10.1103/PhysRevLett.66.3048>
- [24] J. R. Petta, A. C. Johnson, J. M. Taylor, E. A. Laird, A. Yacoby, M. D. Lukin, C. M. Marcus, M. P. Hanson, and A. C. Gossard, “Coherent manipulation of coupled electron spins in semiconductor quantum dots,” *Science*, vol. 309, no. 5744, pp. 2180–2184, 2005. [Online]. Available: <https://www.science.org/doi/abs/10.1126/science.1116955>
- [25] J. M. Elzerman, R. Hanson, L. H. Willems van Beveren, B. Witkamp, L. M. K. Vandersypen, and L. P. Kouwenhoven, “Single-shot read-out of an individual electron spin in a quantum dot,” *Nature*, vol. 430, no. 6998, p. 431–435, Jul. 2004. [Online]. Available: <http://dx.doi.org/10.1038/nature02693>
- [26] D. A. Lidar, I. L. Chuang, and K. B. Whaley, “Decoherence-free subspaces for quantum computation,”

- Phys. Rev. Lett.*, vol. 81, pp. 2594–2597, Sep 1998. [Online]. Available: <https://link.aps.org/doi/10.1103/PhysRevLett.81.2594>
- [27] X. Wang, L. S. Bishop, E. Barnes, J. P. Kestner, and S. D. Sarma, “Robust quantum gates for singlet-triplet spin qubits using composite pulses,” *Phys. Rev. A*, vol. 89, p. 022310, Feb 2014. [Online]. Available: <https://link.aps.org/doi/10.1103/PhysRevA.89.022310>
- [28] E. Kawakami, P. Scarlino, D. R. Ward, F. R. Braakman, D. E. Savage, M. G. Lagally, M. Friesen, S. N. Coppersmith, M. A. Eriksson, and L. M. K. Vandersypen, “Electrical control of a long-lived spin qubit in a si/sige quantum dot,” *Nature Nanotechnology*, vol. 9, no. 9, p. 666–670, Aug. 2014. [Online]. Available: <http://dx.doi.org/10.1038/nnano.2014.153>
- [29] Y. Tokura, W. G. van der Wiel, T. Obata, and S. Tarucha, “Coherent single electron spin control in a slanting zeeman field,” *Phys. Rev. Lett.*, vol. 96, p. 047202, Jan 2006. [Online]. Available: <https://link.aps.org/doi/10.1103/PhysRevLett.96.047202>
- [30] E. Kawakami, T. Jullien, P. Scarlino, D. R. Ward, D. E. Savage, M. G. Lagally, V. V. Dobrovitski, M. Friesen, S. N. Coppersmith, M. A. Eriksson, and L. M. K. Vandersypen, “Gate fidelity and coherence of an electron spin in an si/sige quantum dot with micromagnet,” *Proceedings of the National Academy of Sciences*, vol. 113, no. 42, pp. 11 738–11 743, 2016. [Online]. Available: <https://www.pnas.org/doi/abs/10.1073/pnas.1603251113>
- [31] C. Gidney and M. Ekerå, “How to factor 2048 bit RSA integers in 8 hours using 20 million noisy qubits,” *Quantum*, vol. 5, p. 433, Apr. 2021. [Online]. Available: <https://doi.org/10.22331/q-2021-04-15-433>
- [32] D. Aharonov and M. Ben-Or, “Fault-tolerant quantum computation with constant error rate,” *SIAM Journal on Computing*, vol. 38, no. 4, pp. 1207–1282, 2008. [Online]. Available: <https://doi.org/10.1137/S0097539799359385>
- [33] E. Knill, R. Laflamme, and W. H. Zurek, “Resilient quantum computation,” *Science*, vol. 279, no. 5349, pp. 342–345, 1998. [Online]. Available: <https://www.science.org/doi/abs/10.1126/science.279.5349.342>
- [34] A. Kitaev, “Fault-tolerant quantum computation by anyons,” *Annals of Physics*, vol. 303, no. 1, pp. 2–30, 2003. [Online]. Available: <https://www.sciencedirect.com/science/article/pii/S0003491602000180>
- [35] Y. Kim, C. J. Wood, T. J. Yoder, S. T. Merkel, J. M. Gambetta, K. Temme, and A. Kandala, “Scalable error mitigation for noisy quantum circuits produces competitive expectation values,” *Nature Physics*, vol. 19, no. 5, p. 752–759, Feb. 2023. [Online]. Available: <http://dx.doi.org/10.1038/s41567-022-01914-3>
- [36] S. Endo, S. C. Benjamin, and Y. Li, “Practical quantum error mitigation for near-future applications,” *Phys. Rev. X*, vol. 8, p. 031027, Jul 2018. [Online]. Available: <https://link.aps.org/doi/10.1103/PhysRevX.8.031027>

Appendix A: Hamiltonian Dynamics

1. Exchange interaction

Recall that the Hamiltonian of the exchange interaction is:

$$H_{\text{exc}} = J_{\text{exc}} \mathbf{s}_1 \cdot \mathbf{s}_2. \quad (\text{A1})$$

The expected energy due to this interaction for the different states are:

$$\langle S | H_{\text{exc}} | S \rangle = 0, \quad (\text{A2})$$

$$\langle T_0 | H_{\text{exc}} | T_0 \rangle = \frac{1}{4} J_{\text{exc}}, \quad (\text{A3})$$

$$\langle T_+ | H_{\text{exc}} | T_+ \rangle = \frac{1}{4} J_{\text{exc}}, \quad (\text{A4})$$

$$\langle T_0 | H_{\text{exc}} | T_- \rangle = \frac{1}{4} J_{\text{exc}}. \quad (\text{A5})$$

2. Zeeman interaction

Recall that the Hamiltonian of the Zeeman interaction is:

$$H_Z(\mathbf{B}, \mathbf{r}) = g\mu_B \mathbf{B}(\mathbf{r}, t) \cdot (\mathbf{S}_1(\mathbf{r}_1) + \mathbf{S}_2(\mathbf{r}_2)), \quad (\text{A6})$$

where $\mathbf{B}(\mathbf{r})$ is the external magnetic field which depends on the position \mathbf{r}_i of the i^{th} QD, μ_B is the Bohr magneton and g is the gyromagnetic ratio. The interaction of the singlet state $|S\rangle$ with an external magnetic field is:

$$H_Z(B_x) |S\rangle = g\mu_B [B_{x_1} (X \otimes I) + B_{x_2} (I \otimes X)] |S\rangle \quad (\text{A7})$$

$$= \frac{1}{2} g\mu_B \left[\frac{B_{x_1} (|T_- \rangle - |T_+ \rangle)}{\sqrt{2}} + \frac{B_{x_2} (|T_+ \rangle - |T_- \rangle)}{\sqrt{2}} \right] \quad (\text{A8})$$

$$= \frac{1}{2\sqrt{2}} g\mu_B (B_{x_1} - B_{x_2}) (|T_- \rangle - |T_+ \rangle), \quad (\text{A9})$$

$$H_Z(B_y) |S\rangle = g\mu_B [B_{y_1} (Y \otimes I) + B_{y_2} (I \otimes Y)] |S\rangle \quad (\text{A10})$$

$$= \frac{1}{2} g\mu_B \left[\frac{iB_{y_1} (|T_- \rangle + |T_+ \rangle)}{\sqrt{2}} - \frac{iB_{y_2} (|T_+ \rangle + |T_- \rangle)}{\sqrt{2}} \right] \quad (\text{A11})$$

$$= \frac{i}{2\sqrt{2}} g\mu_B (B_{y_1} - B_{y_2}) (|T_- \rangle + |T_+ \rangle), \quad (\text{A12})$$

$$H_Z(B_z) |S\rangle = g\mu_B [B_{z_1} (Z \otimes I) + B_{z_2} (I \otimes Z)] |S\rangle \quad (\text{A13})$$

$$= \frac{1}{2} g\mu_B \left[\frac{B_{z_1} |T_0 \rangle}{\sqrt{2}} - \frac{B_{z_2} |T_0 \rangle}{\sqrt{2}} \right] \quad (\text{A14})$$

$$= \frac{1}{2} g\mu_B (B_{z_1} - B_{z_2}) |T_0 \rangle. \quad (\text{A15})$$

The interaction of the neutral triplet state $|T_0\rangle$ with an external magnetic field is:

$$H_Z(B_x) |T_0\rangle = g\mu_B [B_{x_1} (X \otimes I) + B_{x_2} (I \otimes X)] |T_0\rangle \quad (\text{A16})$$

$$= \frac{1}{2} g\mu_B \left[\frac{B_{x_1} (|T_- \rangle + |T_+ \rangle)}{\sqrt{2}} + \frac{B_{x_2} (|T_+ \rangle + |T_- \rangle)}{\sqrt{2}} \right] \quad (\text{A17})$$

$$= \frac{1}{2\sqrt{2}} g\mu_B (B_{x_1} + B_{x_2}) (|T_- \rangle + |T_+ \rangle), \quad (\text{A18})$$

$$H_Z(B_y) |T_0\rangle = g\mu_B [B_{y_1} (Y \otimes I) + B_{y_2} (I \otimes Y)] |T_0\rangle \quad (\text{A19})$$

$$= \frac{1}{2} g\mu_B \left[\frac{iB_{y_1} (|T_- \rangle - |T_+ \rangle)}{\sqrt{2}} + \frac{iB_{y_2} (|T_- \rangle - |T_+ \rangle)}{\sqrt{2}} \right] \quad (\text{A20})$$

$$= \frac{i}{2\sqrt{2}} g\mu_B (B_{y_1} + B_{y_2}) (|T_- \rangle - |T_+ \rangle), \quad (\text{A21})$$

$$H_Z(B_z) |T_0\rangle = g\mu_B [B_{z_1} (Z \otimes I) + B_{z_2} (I \otimes Z)] |T_0\rangle \quad (\text{A22})$$

$$= \frac{1}{2} g\mu_B \left[\frac{B_{z_1} |S\rangle}{\sqrt{2}} - \frac{B_{z_2} |S\rangle}{\sqrt{2}} \right] \quad (\text{A23})$$

$$= \frac{1}{2} g\mu_B (B_{z_1} - B_{z_2}) |S\rangle. \quad (\text{A24})$$

The interaction of the positive triplet state $|T_+\rangle$ with an external magnetic field is:

$$H_Z(B_x) |T_+\rangle = g\mu_B [B_{x_1} (X \otimes I) + B_{x_2} (I \otimes X)] |T_+\rangle \quad (\text{A25})$$

$$= \frac{1}{2} g\mu_B \left[\frac{B_{x_1} (|T_0 \rangle - |S \rangle)}{\sqrt{2}} + \frac{B_{x_2} (|T_0 \rangle + |S \rangle)}{\sqrt{2}} \right] \quad (\text{A26})$$

$$= \frac{1}{2\sqrt{2}} g\mu_B [(B_{x_1} + B_{x_2}) |T_0 \rangle - (B_{x_1} - B_{x_2}) |S \rangle], \quad (\text{A27})$$

$$H_Z(B_y) |T_+\rangle = g\mu_B [B_{y_1} (Y \otimes I) + B_{y_2} (I \otimes Y)] |T_+\rangle \quad (\text{A28})$$

$$= \frac{1}{2} g\mu_B \left[\frac{iB_{y_1} (|T_0 \rangle - |S \rangle)}{\sqrt{2}} + \frac{iB_{y_2} (|T_0 \rangle + |S \rangle)}{\sqrt{2}} \right] \quad (\text{A29})$$

$$= \frac{i}{2\sqrt{2}} g\mu_B [(B_{y_1} + B_{y_2}) |T_0 \rangle - (B_{y_1} - B_{y_2}) |S \rangle], \quad (\text{A30})$$

$$H_Z(B_z) |T_+\rangle = g\mu_B [B_{z_1} (Z \otimes I) + B_{z_2} (I \otimes Z)] |T_+\rangle \quad (\text{A31})$$

$$= \frac{1}{2} g\mu_B (B_{z_1} + B_{z_2}) |T_+\rangle. \quad (\text{A32})$$

The interaction of the negative triplet state $|T_-\rangle$ with an external magnetic field is:

ternal magnetic field is:

$$H_Z(B_x) |T_-\rangle = g\mu_B [B_{x_1} (X \otimes I) + B_{x_2} (I \otimes X)] |T_-\rangle \quad (\text{A33})$$

$$= \frac{1}{2} g\mu_B \left[\frac{B_{x_1} (|T_0\rangle + |S\rangle)}{\sqrt{2}} + \frac{B_{x_2} (|T_0\rangle - |S\rangle)}{\sqrt{2}} \right] \quad (\text{A34})$$

$$= \frac{1}{2\sqrt{2}} g\mu_B [(B_{x_1} + B_{x_2}) |T_0\rangle + (B_{x_1} - B_{x_2}) |S\rangle], \quad (\text{A35})$$

$$H_Z(B_y) |T_-\rangle = g\mu_B [B_{y_1} (Y \otimes I) + B_{y_2} (I \otimes Y)] |T_-\rangle \quad (\text{A36})$$

$$= \frac{1}{2} g\mu_B \left[\frac{-iB_{y_1} (|T_0\rangle + |S\rangle)}{\sqrt{2}} + \frac{-iB_{y_2} (|T_0\rangle - |S\rangle)}{\sqrt{2}} \right] \quad (\text{A37})$$

$$= \frac{-i}{2\sqrt{2}} g\mu_B [(B_{y_1} + B_{y_2}) |T_0\rangle + (B_{y_1} - B_{y_2}) |S\rangle], \quad (\text{A38})$$

$$H_Z(B_z) |T_-\rangle = g\mu_B [B_{z_1} (Z \otimes I) + B_{z_2} (I \otimes Z)] |T_-\rangle \quad (\text{A39})$$

$$= \frac{-1}{2} g\mu_B (B_{z_1} + B_{z_2}) |T_-\rangle. \quad (\text{A40})$$

Then the non-zero transitions from the singlet state $|S\rangle$ due to this interactions are:

$$\langle T_+ | H_Z(B_x) | S \rangle = \frac{-1}{2\sqrt{2}} g\mu_B (B_{x_1} - B_{x_2}), \quad (\text{A41})$$

$$\langle T_- | H_Z(B_x) | S \rangle = \frac{1}{2\sqrt{2}} g\mu_B (B_{x_1} - B_{x_2}), \quad (\text{A42})$$

$$\langle T_+ | H_Z(B_y) | S \rangle = \frac{i}{2\sqrt{2}} g\mu_B (B_{y_1} - B_{y_2}), \quad (\text{A43})$$

$$\langle T_- | H_Z(B_y) | S \rangle = \frac{i}{2\sqrt{2}} g\mu_B (B_{y_1} - B_{y_2}), \quad (\text{A44})$$

$$\langle T_0 | H_Z(B_z) | S \rangle = \frac{1}{2} g\mu_B (B_{z_1} - B_{z_2}). \quad (\text{A45})$$

The transitions from the neutral triplet state $|T_0\rangle$ are:

$$\langle T_+ | H_Z(B_x) | T_0 \rangle = \frac{1}{2\sqrt{2}} g\mu_B (B_{x_1} + B_{x_2}), \quad (\text{A46})$$

$$\langle T_- | H_Z(B_x) | T_0 \rangle = \frac{1}{2\sqrt{2}} g\mu_B (B_{x_1} + B_{x_2}), \quad (\text{A47})$$

$$\langle T_+ | H_Z(B_y) | T_0 \rangle = \frac{-i}{2\sqrt{2}} g\mu_B (B_{y_1} + B_{y_2}), \quad (\text{A48})$$

$$\langle T_- | H_Z(B_y) | T_0 \rangle = \frac{i}{2\sqrt{2}} g\mu_B (B_{y_1} + B_{y_2}), \quad (\text{A49})$$

$$\langle S | H_Z(B_z) | T_0 \rangle = \frac{1}{2} g\mu_B (B_{z_1} - B_{z_2}). \quad (\text{A50})$$

The transitions from the neutral triplet state $|T_+\rangle$ are:

$$\langle S | H_Z(B_x) | T_+ \rangle = \frac{-1}{2\sqrt{2}} g\mu_B (B_{x_1} - B_{x_2}), \quad (\text{A51})$$

$$\langle T_0 | H_Z(B_x) | T_+ \rangle = \frac{1}{2\sqrt{2}} g\mu_B (B_{x_1} + B_{x_2}), \quad (\text{A52})$$

$$\langle S | H_Z(B_y) | T_+ \rangle = \frac{-i}{2\sqrt{2}} g\mu_B (B_{y_1} - B_{y_2}), \quad (\text{A53})$$

$$\langle T_0 | H_Z(B_y) | T_+ \rangle = \frac{i}{2\sqrt{2}} g\mu_B (B_{y_1} + B_{y_2}), \quad (\text{A54})$$

$$\langle T_+ | H_Z(B_z) | T_+ \rangle = \frac{1}{2} g\mu_B (B_{z_1} + B_{z_2}). \quad (\text{A55})$$

The transitions from the neutral triplet state $|T_-\rangle$ are:

$$\langle S | H_Z(B_x) | T_- \rangle = \frac{1}{2\sqrt{2}} g\mu_B (B_{x_1} - B_{x_2}), \quad (\text{A56})$$

$$\langle T_0 | H_Z(B_x) | T_- \rangle = \frac{1}{2\sqrt{2}} g\mu_B (B_{x_1} + B_{x_2}), \quad (\text{A57})$$

$$\langle S | H_Z(B_y) | T_- \rangle = \frac{-i}{2\sqrt{2}} g\mu_B (B_{y_1} - B_{y_2}), \quad (\text{A58})$$

$$\langle T_0 | H_Z(B_y) | T_- \rangle = \frac{-i}{2\sqrt{2}} g\mu_B (B_{y_1} + B_{y_2}), \quad (\text{A59})$$

$$\langle T_- | H_Z(B_z) | T_- \rangle = \frac{-1}{2} g\mu_B (B_{z_1} + B_{z_2}). \quad (\text{A60})$$

Finally, the Hamiltonian of a DQD with two electrons with an exchange interaction among them and external magnetic field can be expressed in the $\{|S\rangle, |T_0\rangle, |T_+\rangle, |T_-\rangle\}$ basis as:

$$H_{DQD} = \begin{pmatrix} 0 & \frac{1}{2} g\mu_B \delta B_z & -\frac{1}{2\sqrt{2}} g\mu_B [\delta B_x + i\delta B_y] & \frac{1}{2\sqrt{2}} g\mu_B [\delta B_x - i\delta B_y] \\ \frac{1}{2} g\mu_B \delta B_z & \frac{1}{4} J_{\text{exc}} & \frac{1}{2\sqrt{2}} g\mu_B [B_x + iB_y] & \frac{1}{2\sqrt{2}} g\mu_B [B_x - iB_y] \\ -\frac{1}{2\sqrt{2}} g\mu_B [\delta B_x - i\delta B_y] & \frac{1}{2\sqrt{2}} g\mu_B [B_x - iB_y] & \frac{1}{4} J_{\text{exc}} + \frac{1}{2} g\mu_B B_z & 0 \\ \frac{1}{2\sqrt{2}} g\mu_B [\delta B_x + i\delta B_y] & \frac{1}{2\sqrt{2}} g\mu_B [B_x + iB_y] & 0 & \frac{1}{4} J_{\text{exc}} - \frac{1}{2} g\mu_B B_z \end{pmatrix}, \quad (\text{A61})$$

where $B_x = B_{x_1} + B_{x_2}$, $B_y = B_{y_1} + B_{y_2}$, $B_z = B_{z_1} + B_{z_2}$, $\delta B_x = (B_{x_1} - B_{x_2})$, $\delta B_y = (B_{y_1} - B_{y_2})$ and $\delta B_z = (B_{z_1} - B_{z_2})$.

Appendix B: $SU(2) \otimes SU(2)$ symmetry

The algebra of the direct product of two $SU(2)$ spaces is equal to the direct sum of two subspaces:

$$SU(2) \otimes SU(2) = U(1) \oplus SU(3). \quad (\text{B1})$$

The symmetry $U(1)$ is associated to the singlet, with a symmetric wavefunction in position and asymmetric wavefunction

in spin. The subspace of the singlet $|S\rangle$ does not have spin angular momentum in direction \hat{z} :

$$\langle S | \hat{S}_z | S \rangle = 0, \quad (\text{B2})$$

where \hat{S}_z is the spin angular momentum in direction \hat{z} operator. The symmetry group $SU(3)$ is associated to the triplets, with symmetric wavefunction in spin and an asymmetric wavefunction in position. This subspace has a total spin angular momentum equal to 1 and:

$$\langle T_- | \hat{S}_z | T_- \rangle = -1, \quad (\text{B3})$$

$$\langle T_0 | \hat{S}_z | T_0 \rangle = 0, \quad (\text{B4})$$

$$\langle T_+ | \hat{S}_z | T_+ \rangle = 1. \quad (\text{B5})$$

Then, we can define the Hamiltonian of the system as:

$$H = U(1) \oplus SU(3) = \left(\begin{array}{c|c} U(1) & 0 \\ \hline 0 & SU(3) \end{array} \right). \quad (\text{B6})$$

$U(1)$ only has 1 generator and the generators of $SU(3)$ are given by the Gell-Mann matrices:

$$\begin{aligned} \Lambda_1 &= \begin{pmatrix} 0 & 1 & 0 \\ 1 & 0 & 0 \\ 0 & 0 & 0 \end{pmatrix}, \\ \Lambda_2 &= \begin{pmatrix} 0 & -i & 0 \\ i & 0 & 0 \\ 0 & 0 & 0 \end{pmatrix}, \\ \Lambda_3 &= \begin{pmatrix} 1 & 0 & 0 \\ 0 & -1 & 0 \\ 0 & 0 & 0 \end{pmatrix}, \\ \Lambda_4 &= \begin{pmatrix} 0 & 0 & 1 \\ 0 & 0 & 0 \\ 1 & 0 & 0 \end{pmatrix}, \\ \Lambda_5 &= \begin{pmatrix} 0 & 0 & -i \\ 0 & 0 & 0 \\ -i & 0 & 0 \end{pmatrix}, \\ \Lambda_6 &= \begin{pmatrix} 0 & 0 & 0 \\ 0 & 0 & 1 \\ 0 & 1 & 0 \end{pmatrix}, \\ \Lambda_7 &= \begin{pmatrix} 0 & 0 & 0 \\ 0 & 0 & -i \\ 0 & i & 0 \end{pmatrix}, \\ \Lambda_8 &= \frac{1}{\sqrt{3}} \begin{pmatrix} 1 & 0 & 0 \\ 0 & 1 & 0 \\ 0 & 0 & -2 \end{pmatrix}. \end{aligned} \quad (\text{B7})$$

The energy of each subspace is given by $\eta = \text{diag}(-1, 1, 1, 1)$, which can be seen as the Minkowski metric of the system:

$$H_\eta = \frac{1}{8} J_{\text{exc}} \eta = \frac{1}{8} J_{\text{exc}} \begin{pmatrix} -1 & 0 & 0 & 0 \\ 0 & 1 & 0 & 0 \\ 0 & 0 & 1 & 0 \\ 0 & 0 & 0 & 1 \end{pmatrix}. \quad (\text{B8})$$

Using the Gell-Mann matrices, we are able to reconstruct the Hamiltonian of the subspace related to the triplets. The external magnetic field in the direction \hat{z} splits the space in 3 different states with different spin in \hat{z} S_z , this interaction in

related to $\{\Lambda_1, \Lambda_6\}$. The external magnetic fields in the directions \hat{x} and \hat{y} changes the spin by $\Delta S_z = \pm 1$, so they allow transitions between states with different spin separated by 1 and are related to the matrices $\{\Lambda_1, \Lambda_2, \Lambda_6, \Lambda_7\}$. There are no interactions allowing transition between states with $\Delta S_z = \pm 2$, so the Hamiltonian does not have terms related to $\{\Lambda_4, \Lambda_5\}$. Thus, the Hamiltonian in the basis $\{T_+, T_0, T_-\}$:

$$\begin{aligned} H_{T_0, T_\pm} &= \frac{1}{2} g \mu_B \left(\frac{B_z}{2} \Lambda_3 + \frac{\sqrt{3} B_z}{2} \Lambda_8 \right. \\ &\quad \left. + \frac{1}{\sqrt{2}} B_x \Lambda_1 + \frac{1}{\sqrt{2}} B_x \Lambda_6 + \frac{1}{\sqrt{2}} B_y \Lambda_2 + \frac{1}{\sqrt{2}} B_y \Lambda_7 \right) \quad (\text{B9}) \\ &= \frac{1}{2} g \mu_B \begin{pmatrix} B_z & \frac{1}{\sqrt{2}} (B_x - i B_y) & 0 \\ \frac{1}{\sqrt{2}} (B_x + i B_y) & 0 & \frac{1}{\sqrt{2}} (B_x - i B_y) \\ 0 & \frac{1}{\sqrt{2}} (B_x + i B_y) & -B_z \end{pmatrix}. \end{aligned} \quad (\text{B11})$$

Then, the Hamiltonian of the $SU(2) \otimes SU(2)$ system is given by the block diagonal matrix:

$$H = H_\eta + \begin{pmatrix} 0 & \\ & H_{T_0, T_\pm} \end{pmatrix}. \quad (\text{B12})$$

In such systems we are able to break the symmetry by applying different magnetic fields to each QD, i.e. $B_{i_1} \neq B_{i_2}$ with $i \in \{x, y, z\}$. In this case, each subspace is not protected by this symmetry and transitions between them are possible. The matrix associated to that transitions are given by:

$$\begin{aligned} \Lambda'_1 &= \begin{pmatrix} 0 & 1 & 0 & 0 \\ 1 & 0 & 0 & 0 \\ 0 & 0 & 0 & 0 \\ 0 & 0 & 0 & 0 \end{pmatrix}, \\ \Lambda'_2 &= \begin{pmatrix} 0 & -i & 0 & 0 \\ i & 0 & 0 & 0 \\ 0 & 0 & 0 & 0 \\ 0 & 0 & 0 & 0 \end{pmatrix}, \\ \Lambda'_3 &= \begin{pmatrix} 0 & 0 & 1 & 0 \\ 0 & 0 & 0 & 0 \\ 1 & 0 & 0 & 0 \\ 0 & 0 & 0 & 0 \end{pmatrix}, \\ \Lambda'_4 &= \begin{pmatrix} 0 & 0 & -i & 0 \\ 0 & 0 & 0 & 0 \\ i & 0 & 0 & 0 \\ 0 & 0 & 0 & 0 \end{pmatrix}, \\ \Lambda'_5 &= \begin{pmatrix} 0 & 0 & 0 & 1 \\ 0 & 0 & 0 & 0 \\ 0 & 0 & 0 & 0 \\ 1 & 0 & 0 & 0 \end{pmatrix}, \\ \Lambda'_6 &= \begin{pmatrix} 0 & 0 & 0 & -i \\ 0 & 0 & 0 & 0 \\ 0 & 0 & 0 & 0 \\ i & 0 & 0 & 0 \end{pmatrix}. \end{aligned} \quad (\text{B13})$$

A different magnetic field in each QD breaks the spin-position symmetry, then the interactions between the electrons and the external magnetic field in this situation allows transitions between subspaces $U(1)$ and $SU(3)$. An external field with $\delta B_z \neq 0$ does not give an angular momentum in the \hat{z} direction, but it allows transitions between the states $|S\rangle$ and $|T_0\rangle$. In the situation of $\delta B_x, \delta B_y \neq 0$, transitions between states in

different subspaces and with different angular momentum are allowed. The Hamiltonian of the interactions which break the

symmetry is given by:

$$\begin{aligned} H_{BS} &= \frac{1}{2}g\mu_b(\delta B_z\Lambda'_3 - \frac{1}{\sqrt{2}}\delta B_x\Lambda'_1 + \frac{1}{\sqrt{2}}\delta B_x\Lambda'_3 \\ &\quad + \frac{1}{\sqrt{2}}\delta B_y\Lambda'_2 + \frac{1}{\sqrt{2}}\delta B_y\Lambda'_6) \\ &= \frac{1}{2}g\mu_b \begin{pmatrix} 0 & \frac{-1}{\sqrt{2}}(\delta B_x + i\delta B_y) & \delta B_z & \frac{1}{\sqrt{2}}(\delta B_x - i\delta B_y) \\ \frac{-1}{\sqrt{2}}(\delta B_x - i\delta B_y) & 0 & 0 & 0 \\ \delta B_z & 0 & 0 & 0 \\ \frac{1}{\sqrt{2}}(\delta B_x + i\delta B_y) & 0 & 0 & 0 \end{pmatrix}. \end{aligned} \quad (\text{B14})$$

And the Hamiltonian of a DQD is:

$$\begin{aligned} H &= H_\eta + \begin{pmatrix} 0 & \\ & H_{T_0, T_\pm} \end{pmatrix} + H_{BS} \\ &= \frac{1}{2}g\mu_B \begin{pmatrix} -\frac{1}{4g\mu_B}J_{\text{exc}} & \frac{-1}{\sqrt{2}}(\delta B_x + i\delta B_y) & \delta B_z & \frac{1}{\sqrt{2}}(\delta B_x - i\delta B_y) \\ \frac{-1}{\sqrt{2}}(\delta B_x - i\delta B_y) & \frac{1}{4g\mu_B}J_{\text{exc}} + B_z & \frac{1}{\sqrt{2}}(B_x - iB_y) & 0 \\ \delta B_z & \frac{1}{\sqrt{2}}(B_x + iB_y) & \frac{1}{4g\mu_B}J_{\text{exc}} & \frac{1}{\sqrt{2}}(B_x - iB_y) \\ \frac{1}{\sqrt{2}}(\delta B_x + i\delta B_y) & 0 & \frac{1}{\sqrt{2}}(B_x + iB_y) & \frac{1}{4g\mu_B}J_{\text{exc}} - B_z \end{pmatrix}. \end{aligned} \quad (\text{B15})$$

It is important to note that the sign of the exchange coupling J_{exc} does not change the dynamics of the DQD system since it has inversion symmetry. Once the Lie algebra and its generators beyond our quantum system are defined, we are able

to study the dynamics of a DQD using rotation operators. Following the discussion in Sec. II C and using Eq. 33, we can represent a general rotation as:

$$\begin{aligned} R(H, \tau_g) &= \mathcal{T} \left\{ \exp \left(\frac{-i}{2} \int_0^{\tau_g} dt H(t) \right) \right\} \\ &= \mathcal{T} \left\{ \exp \left(\frac{-i}{2} \int_0^{\tau_g} dt \left[\frac{1}{8}J_{\text{exc}}\eta + \frac{1}{2}g\mu_B \left(\frac{B_z}{2}\Lambda_3 + \frac{\sqrt{3}B_z}{2}\Lambda_8 + \frac{1}{\sqrt{2}}B_x\Lambda_1 + \frac{1}{\sqrt{2}}B_x\Lambda_6 + \frac{1}{\sqrt{2}}B_y\Lambda_2 + \frac{1}{\sqrt{2}}B_y\Lambda_7 \right. \right. \right. \\ &\quad \left. \left. \left. + \frac{1}{2}g\mu_b \left(\delta B_z\Lambda'_3 - \frac{1}{\sqrt{2}}\delta B_x\Lambda'_1 + \frac{1}{\sqrt{2}}\delta B_x\Lambda'_3 + \frac{1}{\sqrt{2}}\delta B_y\Lambda'_2 + \frac{1}{\sqrt{2}}\delta B_y\Lambda'_6 \right) \right] \right) \right\}, \end{aligned} \quad (\text{B16})$$

where the rotation axis \hat{r} is given by:

$$\hat{r} = \frac{H(t)}{\sqrt{\left(\frac{1}{8}J_{\text{exc}} \right)^2 + \left(\frac{1}{2}g\mu_B \right)^2 \left(\left(\frac{B_z}{2} \right)^2 + \left(\frac{\sqrt{3}B_z}{2} \right)^2 + 2 \left(\frac{1}{\sqrt{2}}B_x \right)^2 + 2 \left(\frac{1}{\sqrt{2}}B_y \right)^2 + (\delta B_z)^2 + 2 \left(\frac{1}{\sqrt{2}}\delta B_x \right)^2 + 2 \left(\frac{1}{\sqrt{2}}\delta B_y \right)^2 \right)}. \quad (\text{B18})$$

Appendix C: Mathematical rotations and other encoded spin qubits

1. Rotations of a ST_0 qubit

Mathematically, rotations of a ST_0 qubit can be represented as:

$$\hat{\sigma}^x = S_1^z - S_2^z, \quad (\text{C1})$$

$$\hat{\sigma}^y = 2\hat{z} \cdot \mathbf{S}_2 \times \mathbf{S}_1, \quad (\text{C2})$$

$$\hat{\sigma}^z = 2(\mathbf{S}_1 \cdot \mathbf{S}_2) - S_1^z S_2^z. \quad (\text{C3})$$

2. Other spin qubits encoded in a 2-electron DQD system

a. Flip-Flop qubits

The Flip-Flop qubits are encoded within a DQD system, the computational basis is given by:

$$|0\rangle = |\uparrow\downarrow\rangle = \frac{1}{\sqrt{2}}(|S\rangle + |T_0\rangle), \quad (\text{C4})$$

$$|1\rangle = |\downarrow\uparrow\rangle = \frac{1}{\sqrt{2}}(|S\rangle - |T_0\rangle). \quad (\text{C5})$$

In this case, the energy levels are a linear combination of the singlet and T_0 triplet. The rotations are controlled by changing the exchange coupling with the detuning ε and by the external magnetic fields:

$$\hat{\sigma}^x = 2(\mathbf{S}_1 \cdot \mathbf{S}_2) - S_1^z S_2^z, \quad (\text{C6})$$

$$\hat{\sigma}^y = 2\hat{z} \cdot \mathbf{S}_2 \times \mathbf{S}_1, \quad (\text{C7})$$

$$\hat{\sigma}^z = S_1^z - S_2^z. \quad (\text{C8})$$

3. ST_{\pm} Qubits

The ST_+ qubits are encoded within a DQD system, the computational basis is given by:

$$|0\rangle = |S\rangle, \quad (\text{C9})$$

$$|1\rangle = |\uparrow\uparrow\rangle \text{ or } |\downarrow\downarrow\rangle. \quad (\text{C10})$$

The energy splitting between the computational basis is given by the gradient of the external magnetic field ΔB_z . The rotations are controlled by the potential of each QD and the potential of the barrier, to tune the exchange coupling, and by the external magnetic field:

$$\hat{\sigma}^x = (S_2^x - S_1^x) / \sqrt{2} + \sqrt{2}\hat{y} \cdot \mathbf{S}_2 \times \mathbf{S}_1 \quad (\text{C11})$$

$$\hat{\sigma}^y = (S_1^y - S_2^y) / \sqrt{2} + \sqrt{2}\hat{x} \cdot \mathbf{S}_1 \times \mathbf{S}_2 \quad (\text{C12})$$

$$\hat{\sigma}^z = -(S_1^z + S_2^z) / 2 - \mathbf{S}_1 \cdot \mathbf{S}_2 - S_1^z S_2^z. \quad (\text{C13})$$

Appendix D: Dyson series

$$\hat{U}(t, t_0) \approx 1 - \frac{i}{\hbar} \int_{t_0}^t dt_1 H_I(t) \quad (\text{D1})$$

$$+ \left(\frac{-i}{\hbar}\right)^2 \int_{t_0}^t dt_1 \int_{t_0}^{t_1} dt_2 H_I(t_1) H_I(t_2), \quad (\text{D2})$$

where H_I is formed by the off-diagonal terms of H , the interaction terms. The Hamiltonian is given in Eq. B15 and we assume that the pulses have a constant value during the gate:

$$\hat{U}_I(t, t_0) \approx 1 + \frac{-i}{\hbar} \int_{t_0}^t dt_1 H_I(t) \quad (\text{D3})$$

$$+ \left(\frac{-i}{\hbar}\right)^2 \int_{t_0}^t dt_1 \int_{t_0}^{t_1} dt_2 H_I(t_1) H_I(t_2) \quad (\text{D4})$$

$$= 1 - \frac{i}{\hbar} H_I t + \frac{1}{2} \left(\frac{-i}{\hbar}\right)^2 (H_I t)^2. \quad (\text{D5})$$

If the initial state is $|S\rangle$, the first order in the Dyson series terms would be given by $\langle \psi | \int_{t_0}^t dt_1 H_I(t_1) | S \rangle$:

$$A_{S \rightarrow S}^I = 0, \quad (\text{D6})$$

$$A_{S \rightarrow T_0}^I = \frac{1}{2} g \mu_B \delta B_z t, \quad (\text{D7})$$

$$A_{S \rightarrow T_+}^I = \frac{1}{2} g \mu_B \left[\frac{-1}{\sqrt{2}} (\delta B_x - i \delta B_y) \right] t, \quad (\text{D8})$$

$$A_{S \rightarrow T_-}^I = \frac{1}{2} g \mu_B \left[\frac{1}{\sqrt{2}} (\delta B_x + i \delta B_y) \right] t. \quad (\text{D9})$$

The second order terms of the dyson series that come back to the state $|T_0\rangle$ are given by $\langle T_0 | \int_{t_0}^t dt_1 \int_{t_0}^{t_1} dt_2 H_I(t_1) H_I(t_2) | S \rangle$:

$$A_{S \rightarrow S \rightarrow T_0}^I = 0, \quad (\text{D10})$$

$$A_{S \rightarrow T_0 \rightarrow T_0}^I = 0, \quad (\text{D11})$$

$$A_{S \rightarrow T_+ \rightarrow T_0}^I = \frac{-1}{8} (g \mu_B)^2 (\delta B_x - i \delta B_y) (B_x + i B_y) \frac{t^2}{2}, \quad (\text{D12})$$

$$A_{S \rightarrow T_- \rightarrow T_0}^I = \frac{1}{8} (g \mu_B)^2 (\delta B_x + i \delta B_y) (B_x - i B_y) \frac{t^2}{2}. \quad (\text{D13})$$

Then the time evolution operator in the interaction picture to go from the state $|S\rangle$ to the state $|T_0\rangle$ up to second order is:

$$\hat{U}_I^{S \rightarrow T_0}(t, 0) \approx \frac{-it}{\hbar} \frac{1}{2} g \mu_B \delta B_z + \frac{1}{2} \left(\frac{-it}{\hbar}\right)^2 \left(\frac{1}{2} g \mu_B\right)^2 \left(\frac{-1}{2} (\delta B_x - i \delta B_y) \cdot (B_x + i B_y) + \frac{1}{2} (\delta B_x + i \delta B_y) \cdot (B_x - i B_y)\right) \quad (\text{D14})$$

$$= \frac{-it}{\hbar} \frac{1}{2} g \mu_B \delta B_z - i \left(\frac{t}{\hbar}\right)^2 \left(\frac{1}{2\sqrt{2}} g \mu_B\right)^2 (\delta B_x B_y - \delta B_y B_x) \quad (\text{D15})$$

We can compute the evolution up to second order from the state $|T_0\rangle$ to $|S\rangle$ in the same way. Since $\langle S | H_I(t) | T_0 \rangle =$

$\left(\langle T_0 | H_I^\dagger(t) | S \rangle\right)^\dagger = (\langle T_0 | H_I(t) | S \rangle)^\dagger$ the evolution is given by

the same expression. The effective amplitude of the transition from the state $|S\rangle$ to $|T_0\rangle$ in the Schrödinger picture is given by:

$$A_{|S\rangle\rightarrow|T_0\rangle} = A_{|S\rangle\rightarrow|T_0\rangle}^0 + A_{|S\rangle\rightarrow|T_0\rangle}^1 + A_{|S\rangle\rightarrow|T_0\rangle}^2, \quad (\text{D16})$$

where

$$A_{|S\rangle\rightarrow|T_0\rangle}^0 = 0 \quad (\text{D17})$$

$$A_{|S\rangle\rightarrow|T_0\rangle}^1 = \frac{1}{2}g\mu_B\delta B_z \quad (\text{D18})$$

To compute the second order amplitude, we have to start with the integral amplitude in the interaction picture:

$$A_{|S\rangle\rightarrow|T_0\rangle}^{I;2} = \sum_{m=T_{\pm}} \left(\frac{-i}{\hbar}\right)^2 \int_{t_0}^t dt_1 \int_{t_0}^{t_1} dt_2 \langle T_0 | H_I(t_1) | m \rangle \langle m | H_I(t_2) | S \rangle, \quad (\text{D19})$$

and rewrite it in the Schrödinger picture:

$$A_{|S\rangle\rightarrow|T_0\rangle}^{S;2} = \sum_{m=T_{\pm}} \left(\frac{-i}{\hbar}\right)^2 \int_{t_0}^t dt_1 \int_{t_0}^{t_1} dt_2 \langle T_0 | H_I(t_1) | m \rangle \langle m | H_I(t_2) | S \rangle e^{-i(\lambda_{|m\rangle} - \lambda_{|T_0\rangle})t_1/\hbar} e^{-i(\lambda_{|S\rangle} - \lambda_{|m\rangle})t_2/\hbar}. \quad (\text{D20})$$

Then, we solve it from $t_0 = -\infty$ to t :

$$A_{|S\rangle\rightarrow|T_0\rangle}^{S;2} = - \sum_{m=T_{\pm}} \frac{\langle T_0 | H_I | m \rangle \langle m | H_I | S \rangle}{(\lambda_{|S\rangle} - \lambda_{|m\rangle})(\lambda_{|S\rangle} - \lambda_{|T_0\rangle})} \quad (\text{D21})$$

Finally, the second order transition amplitude from the state $|S\rangle$ to $|T_0\rangle$ is given by:

$$A_{|S\rangle\rightarrow|T_0\rangle}^2 = (\lambda_{|T_0\rangle} - \lambda_{|S\rangle}) A_{|S\rangle\leftrightarrow|T_0\rangle}^{S;2} = \sum_{m=T_{\pm}} \frac{\langle T_0 | H_I | m \rangle \langle m | H_I | S \rangle}{\lambda_{|S\rangle} - \lambda_{|m\rangle}} \quad (\text{D22})$$

Similarly, we can compute the second order transition amplitude from the state $|T_0\rangle$ to $|S\rangle$:

$$A_{|T_0\rangle\rightarrow|S\rangle}^2 = \sum_{m=T_{\pm}} \frac{\langle S | H_I | m \rangle \langle m | H_I | T_0 \rangle}{\lambda_{|T_0\rangle} - \lambda_{|m\rangle}} \quad (\text{D23})$$